# Conformational Changes and Anion−Cation Interactions in Palladium-Cyclometalated BINAP and Chiraphos Cationic Complexes. A Structural Study via NMR and X-ray Methods

Devendrababu Nama, Pietro Butti, and Paul S. Pregosin*

*Laboratory of Inorganic Chemistry, ETH Zurich, Zürich CH-8093, Switzerland*

*Received March 28, 2007*

The cyclometalated Pd complexes [Pd{(A or B)$C_6H_3CH$═N(*p*-$CH_3C_6H_4$)}(BINAP)](X) (**8**−**13**; X = $PF_6^-$, $BArF^-$, $CF_3SO_3^-$, A, B = meta or para ring substituent), [Pd{($C_6H_4CH(CH_3)N(CH_3)_2$)}{(*S*)- or (*R*)-BINAP)}]($CF_3SO_3$) (**14a**,**b**), and [Pd{($C_6H_4CH(CH_3)N(CH_3)_2$)}{(*S*,*S*)- or (*R*,*R*)-Chiraphos)}]($CF_3SO_3$) (**15a**,**b**) have been prepared, and five of these have been studied by X-ray diffraction. NMR Overhauser measurements reveal that the chiral cyclometalated amine chelate senses the change in the chirality, for both the BINAP and the Chiraphos auxiliaries, and responds by a conformational adjustment of the ring. $^1H$,$^{19}F$-HOESY data for both **14** and **15** suggest differences between the diastereomers **14a**,**b** (and **15a**,**b**). PGSE diffusion data for these salts are reported.

## Introduction

An increasing number of homogeneous catalysts contain cationic transition-metal salts, e.g., in Pd-[1,2] or Ru-catalyzed[3] allylic alkylation, Pd-catalyzed copolymerization,[4] Ru-catalyzed Diels−Alder chemistry,[5] or Ir-catalyzed hydrogenation.[6] Occasionally, one finds reports of an anion effect on the reaction rate, the nature of the product, or both.[7−12] Normally, there is either a vague or no explanation for this type of anion effect.

Recently, Marks and Macchioni[13] have studied how boron reagents generate and activate Ti and Zr polymerization catalysts by investigating the nature of the ion pairs formed. Their explanation involves, partially, inner sphere vs outer sphere ion pairs. However, generally speaking, it is also possible that an anion may (a) be a complexed ligand, (b) simply sit in an area through which a reagent must pass in order to reach the metal center,[5b,14] or (c) simply slow the deactivation of a complex via steric effects (e.g. steric hindrance to cluster formation).[15]

There are not many ways of monitoring how anions such as $CF_3SO_3^-$, $PF_6^-$ and $BF_4^-$ interact with metals. However, several groups have settled on a combination of NMR diffusion and $^1H$,$^{19}F$-HOESY measurements as the methods of choice.[16−20] The former allows one to estimate the extent of ion pairing, whereas the latter permits a qualitative placement of the anion in three-dimensional space. In contrast to the case for conductivity measurements, there is no solvent polarity limitation using this NMR approach. Further, as long as the pertinent NMR resonances are well resolved, one can obtain results for mixtures containing a number of species.

Although the anions do not usually markedly affect the ee's in enantioselective catalytic reactions,[5,6] it would be useful to know if (and how) the nature of a chiral pocket changes the cation/anion interaction. To this end, we have prepared a number of cyclometalated monocationic palladium complexes containing

(1) Helmchen, G.; Pfaltz, A. *Acc. Chem. Res.* **2000**, *33*, 336−345.
(2) Helmchen, G. *J. Organomet. Chem.* **1999**, *576*, 203−214.
(3) Trost, B. M.; Fraisse, P. L.; Ball, Z. T. A. *Angew. Chem., Int. Ed.* **2003**, *41*, 1059−1061. Trost, B. M.; Fraisse, P. L.; Ball, Z. T. *Angew. Chem., Int. Ed.* **2002**, *41*, 1059−1061. Hermatschweiler, R.; Fernandez, I.; Breher, F.; Pregosin, P. S.; Veiros, L. F.; Calhorda, M. J. *Angew. Chem., Int. Ed.* **2005**, *44*, 4397−4400.
(4) Gsponer, A.; Consiglio, G. *Helv. Chim. Acta* **2003**, *86*, 2170−2172. Sirbu, D.; Consiglio, G.; Milani, B.; Kumar, P. G. A.; Pregosin, P. S.; Gischig, S. *J. Organomet. Chem.* **2005**, *690*, 2254−2262.
(5) (a) Kundig, E. P.; Saudan, C. M.; Bernardinelli, G. H. *Angew. Chem.* **1999**, *111*, 1298−1301. (b) Kumar, P. G. A.; Pregosin, P. S.; Vallet, M.; Bernardinelli, G.; Jazzar, R. F.; Viton, F.; Kundig, E. P. *Organometallics* **2004**, *23*, 5410−5418.
(6) Smidt, S. P.; Zimmermann, N.; Studer, M.; Pfaltz, A. *Chem. Eur. J.* **2004**, *10*, 4685−4693. Mazet, C.; Smiidt, S. P.; Meuwly, M.; Pfaltz, A. *J. Am. Chem. Soc.* **2004**, *126*, 14176−14181. McIntyre, S.; Hormann, E.; Menges, F.; Smidt, S. P.; Pfaltz, A. *Adv. Synth. Catal.* **2005**, *347*, 282−288.
(7) Lautens, M.; Fagnou, K.; Yang, D. Q. *J. Am. Chem. Soc.* **2003**, *125*, 14884−14892.
(8) Fagnou, K.; Lautens, M. *Angew. Chem., Int. Ed.* **2002**, *41*, 27−47.
(9) Krossing, I.; Raabe, I. *Angew. Chem., Int. Ed.* **2004**, *43*, 2066−2090.
(10) Lancaster, N. L.; Welton, T. *J. Org. Chem.* **2004**, *69*, 5986−5992.
(11) Faller, J. W.; Fontaine, P. P. *Organometallics* **2005**, *24*, 4132−4138.
(12) Semeril, D.; Bruneau, C.; Dixneuf, P. H. *Adv. Synth. Catal.* **2002**, *344*, 585−595.
(13) Stahl, N. G.; Zuccaccia, C.; Jensen, T. R.; Marks, T. J. *J. Am. Chem. Soc.* **2003**, *125*, 5256−5257. Zuccaccia, C.; Stahl, N. G.; Macchioni, A.; Chen, M. C.; Roberts, J. A.; Marks, T. J. *J. Am. Chem. Soc.* **2004**, *126*, 1448−1464. Chen, M. C.; Roberts, J. A. S.; Marks, T. J. *J. Am. Chem. Soc.* **2004**, *126*, 4605−4625.
(14) Kumar, P. G. A.; Pregosin, P. S.; Schmid, T. M.; Consiglio, G. *Magn. Reson. Chem.* **2004**, *42*, 795−800.
(15) Martinez-Viviente, E.; Pregosin, P. S. *Inorg. Chem.* **2003**, *42*, 2209−2214.
(16) (a) Pregosin, P. S. *Prog. Nucl. Magn. Reson. Spectrosc.* **2006**, *49*, 261−288. (b) Pregosin, P. S.; Kumar, P. G. A.; Fernandez, I. *Chem. Rev.* **2005**, *105*, 2977−2998. (c) Pregosin, P. S.; Martinez-Viviente, E.; Kumar, P. G. A. *Dalton Trans.* **2003**, 4007−4014.
(17) (a) Pettinari, C.; Pettinari, R.; Marchetti, F.; Macchioni, A.; Zuccaccia, D.; Skelton, B. W.; White, A. H. *Inorg. Chem.* **2007**, *46*, 896−906. (b) Ciancaleoni, G.; Di Maio, I.; Zuccaccia, D.; Macchioni, A. *Organometallics* **2007**, *26*, 489−496. (c) Zuccaccia, D.; Busetto, L.; Cassani, M. C.; Macchioni, A.; Mazzoni, R. *Organometallics* **2006**, *25*, 2201−2208. (d) Zuccaccia, D.; Bellachioma, G.; Cardaci, G.; Zuccaccia, C.; Macchioni, A. *Dalton Trans.* **2006**, 1963−1971. (e) Zuccaccia, C.; Bellachioma, G.; Cardaci, G.; Macchioni, A.; Binotti, B.; Carfagna, C. *Helv. Chim. Acta* **2006**, *89*, 1524−1546. (f) Macchioni, A. *Chem. Rev.* **2005**, *105*, 2039−2073. (g) Zuccaccia, C.; Macchioni, A.; Orabona, I.; Ruffo, F. *Organometallics* **1999**, *18*, 4367−4372 and references therein.
(18) Keresztes, I.; Williard, P. G. *J. Am. Chem. Soc.* **2000**, *122*, 10228−10229.
(19) Branda, T.; Cabrita, E. J.; Berger, S. *Prog. Nucl. Magn. Reson. Spectrosc.* **2005**, *46*, 159−196.
(20) Cohen, Y.; Avram, L.; Frish, L. *Angew. Chem., Int. Ed.* **2005**, *44*, 520−554.

10.1021/om700299b CCC: $37.00 © 2007 American Chemical Society
Publication on Web 08/29/2007

**Scheme 1**

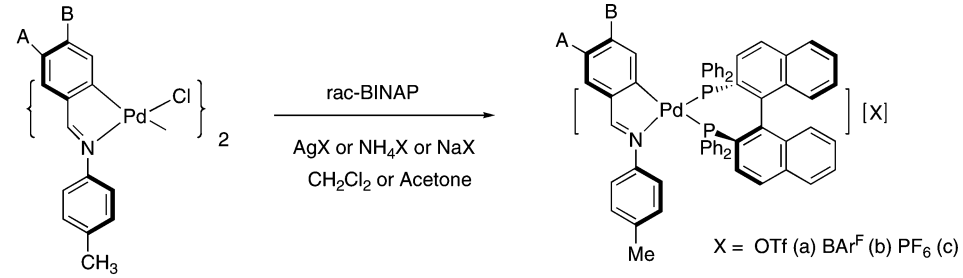


| | A | B |
|---|---|---|
| **1.** | Me | H |
| **2.** | Cl | H |
| **3.** | $NO_2$ | H |
| **4.** | OMe | H |
| **5.** | H | Me |
| **6.** | H | $NO_2$ |

| | A | B |
|---|---|---|
| **8.** | Me | H |
| **9.** | Cl | H |
| **10.** | $NO_2$ | H |
| **11.** | OMe | H |
| **12.** | H | Me |
| **13.** | H | $NO_2$ |

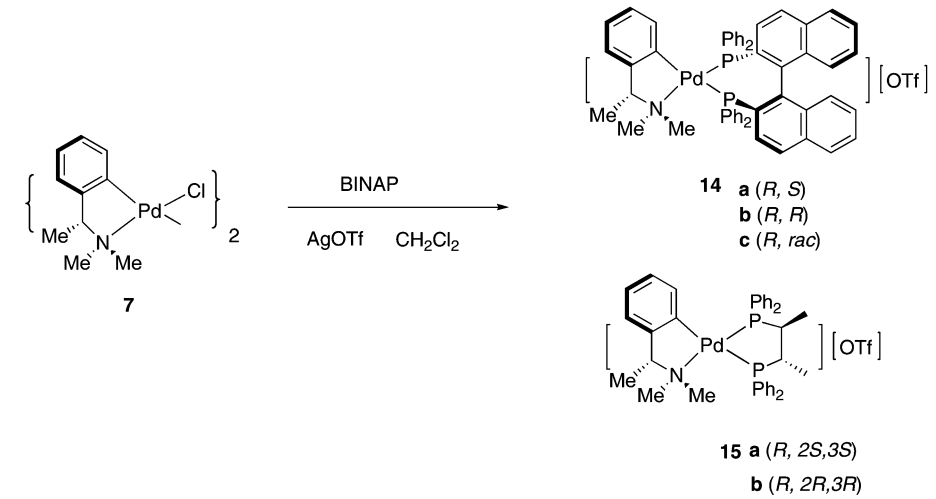


(primarily) various BINAP enantiomers and, to a lesser extent, the two commercially available optically pure 2,3-bis(diphenylphosphino)butane (Chiraphos) ligands (see Scheme 1). We have chosen two different, but well-known, types of cyclometalated C,N-chelates and show these precursors as I and II.

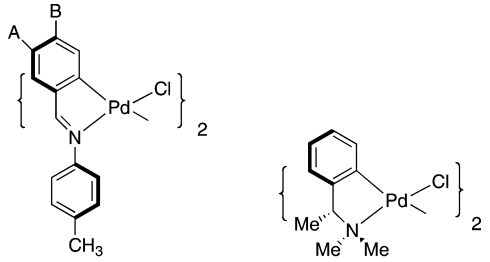

I II

Set I was chosen as a general model for II and because the substituents A and B could be varied. Precursor II was selected because of its asymmetric nature and the commercial availability of, for example, the enantiopure *R* configuration. The reaction of II with an enantiopure P chelate (*R* or *S* of the bidentate phosphine) will afford cationic diastereomers that might differ in their interactions with the anions. N,C-cyclopalladated compounds of various types have been known for more than 30 years,[21−23] can be modified to P,C-analogues,[24,25] and have been used in a variety of applications: e.g., for chiral recognition,[26] as a template,[27] or in asymmetric synthesis.[28]

We report here aspects of the solid-state structures (for five of these salts), NMR diffusion characteristics, and most important, the solution structures, via $^1$H,$^1$H-NOESY and $^1$H,$^{19}$F-HOESY data, for several $CF_3SO_3^-$ (triflate) salts. The observed selective Overhauser results on the diastereomeric triflate salts

(21) Dehand, J.; Pfeffer, M. Cyclometallated Compounds. *Coord. Chem. Rev.* **1976**, *18*, 327−352. Pfeffer, M.; Fischer, J.; Mitschler, A.; Ricard, L. *J. Am. Chem. Soc.* **1980**, *102*, 6338. Pfeffer, M. *Recl. Trav. Chim. Pays-Bas* **1990**, *109*, 567 and references therein.

(22) Ryabov, A. D. *Chem. Rev.* **1990**, *90*, 403.

(23) Espinet, P.; Esteruelas, M. A.; Oro, L. A.; Serrano, J. L.; Sola, E. *Coord. Chem. Rev.* **1992**, *15*, 215 and references therein.

(24) Li, Y.; Tan, G.-K.; Koh, L. L.; Vittal, J. J.; Leung, P. H. *Inorg. Chem.* **2005**, *44*, 9874−9886.

(25) Albinati, A.; Affolter, S.; Pregosin, P. S. *Organometallics* **1990**, *9*, 379−387.

(26) (a) Miyashita, A.; Takaya, H.; Souchi, T.; Noyori, R. *Tetrahedron* **1984**, *40*, 1245−1253. (b) Lopez, C.; Bosque, R.; Sainz, D.; Solans, X.; Font-Bardia, M. *Organometallics* **1997**, *16*, 3261−3266. (c) Roberts, N. K.; Wild, S. B. *J. Am. Chem. Soc.* **1979**, *101*, 6254.

(27) Qin. Y.; Lang, H.; Vittal, J. J.; Tan, G.-K.; Selvaratnam, S.; White, A. J. P.; Williams, D. J.; Leung, P.-H. *Organometallics* **2003**, *22*, 3944−3950.

(28) Kirsch, S. F.; Overman, L. E. *J. Am. Chem. Soc.* **2005**, *127*, 2866−2867. Overman, L. E.; Remarchuk,. T. P. *J. Am. Chem. Soc.* **2002**, *124*, 12−13.

clearly demonstrate that the anion recognizes, and adjusts to, the chiral pocket.

## Results and Discussion

The new complexes were prepared by reaction of the appropriate bidentate phosphine with the known cyclometalated chloro-bridged Pd(II) species, in the presence of AgX, as indicated in Scheme 1. These salts were characterized via NMR, X-ray, mass spectrometric, and microanalytical methods.

The $^{31}$P NMR spectra for the new salts showed AX spin systems with two very different phosphorus chemical shifts: e.g., for **12a**, P1 at 40.8 ppm and P2 at 13.3 ppm ($^2J_{PP} = 47.8$ Hz). The lower frequency resonance, P2, can be assigned to the P atom trans to the $\sigma$-bound carbon donor. The $^1$H spectra for the Schiff base complexes showed the imine proton at relatively high frequency, e.g., for **12a**, H7 at 8.05 ppm, whereas the diastereomeric dimethylamino salts revealed three well-resolved methyl signals in addition to the aliphatic methine CH absorption.

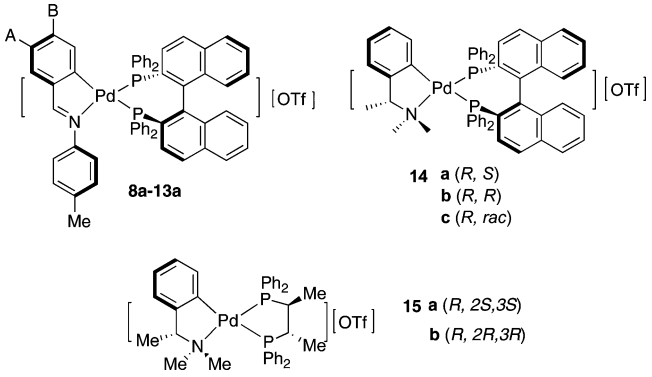


As expected, the $^{13}$C chemical shifts for the imine complexes **8**−**15** show that the Pd-bound carbon atom appears at relatively high frequency[29−31] and senses the presence of the A substituent, in that this resonance is shifted markedly to high frequency[30−32] with A = $NO_2$ and to lower frequency with A = MeO (see Table 1). Interestingly, $^2J$(P,C) is not markedly affected by the A or B groups.

**Solid-State Structures.** Table 2 gives selected bond lengths (Å) and bond angles (deg) for the Pd(*rac*-BINAP) $CF_3SO_3^-$ salts of the imine derivatives **8a** and **10a**, as well as for the Pd(*R*-cyclometalated amine)((*R*)-BINAP) diastereomer **14b** and the *R*, *rac* combination **14c**. The first descriptor refers to the amine (and is always *R*) and the second to the phosphine. Figures 1−4 show ORTEP views of these salts. The X-ray data for a fifth salt, **15a**, afforded a clear result for the cation (see Figure 5); however, a suitable solution for the disorder in the anion could not be found.

The four cations **8a**, **10a**, and **14b**,**c** reveal a local distorted-square-planar geometry about the palladium atom. Within each cation, the two Pd−P separations are quite different. The Pd−P distance trans to the carbon is seen to be ca. 0.10−0.15 Å, longer than that found for the Pd−P distance trans to the nitrogen atom. We note that for **14b** the Pd−P separation of ca. 2.42 Å lies at the upper end of the range for this type of bond. Moreover, this value is significantly larger than the analogous distance found in **10a**, ca. 2.36 Å, suggesting a stronger trans influence for the aliphatic carbon donor. The Pd−N and Pd−C bond lengths are consistent with the literature values.[33] As expected, the N−Pd−C angle from the five-membered ring is relatively small, ca. 79−80°, whereas the P−Pd−P angles are all slightly larger than 90°. This latter angle is typical for the BINAP chelate.[34] Figures

**Table 1. $^{13}$C NMR Data for the Bound C Atom $C_1$ in Complexes 8a−15a[b]**

| A | B | δ ($^{13}$C1) | $^2J_{CP}$ trans | $^2J_{CP}$ cis |
|---|---|---|---|---|
| Me | H | 164.8 | 122.0 | 5.5 |
| Cl | H | 166.0 | 124.0 | 5.7 |
| $NO_2$ | H | 177.2 | 123.3 | 4.6 |
| OMe | H | 158.6 | 126.0 | 5.8 |
| H | Me | 168.3 | 125.0 | 6.0 |
| H | $NO_2$ | 169.2 | 125.2 | 4.8 |

| comp | δ ($^{13}$C1) | | |
|---|---|---|---|
| **14a**[a] | 162.1 | 108.9 | 5.0 |
| **15a** | 158.9 | 111.0 | 4.8 |

[a] 125.8 MHz. [b] Conditions unless other stated: $CD_2Cl_2$, 100 MHz, 298 K.

**Table 2. Bond Lengths (Å) and Bond Angles (deg) for 8a, 10a, and 14b,c**

| | | | |
|---|---|---|---|
| Complex **8a** | | | |
| Pd(1)−C(1) | 2.065(4) | Pd(1)−P(1) | 2.2601(10) |
| Pd(1)−N(1) | 2.124(3) | Pd(1)−P(2) | 2.3876(10) |
| C(1)−Pd(1)−N(1) | 80.11(14) | C(1)−Pd(1)−P(2) | 160.27(11) |
| C(1)−Pd(1)−P(1) | 92.16(11) | N(1)−Pd(1)−P(2) | 98.50(9) |
| N(1)−Pd(1)−P(1) | 166.94(9) | P(1)−Pd(1)−P(2) | 92.31(3) |
| Complex **10a** | | | |
| Pd(1)−C(1) | 2.069(2) | Pd(1)−P(2) | 2.2670(6) |
| Pd(1)−N(1) | 2.134(2) | Pd(1)−P(1) | 2.3643(6) |
| C(1)−Pd(1)−N(1) | 80.39(9) | C(1)−Pd(1)−P(1) | 166.13(7) |
| C(1)−Pd(1)−P(2) | 92.96(7) | N(1)−Pd(1)−P(1) | 96.97(6) |
| N(1)−Pd(1)−P(2) | 167.86(6) | P(2)−Pd(1)−P(1) | 91.86(2) |
| Complex **14b** | | | |
| Pd(1)−C(1) | 2.026(3) | Pd(1)−P(2) | 2.2616(6) |
| Pd(1)−N(1) | 2.192(2) | Pd(1)−P(3) | 2.4182(7) |
| C(1)−Pd(1)−N(1) | 78.74(10) | C(1)−Pd(1)−P(3) | 171.30(9) |
| C(1)−Pd(1)−P(2) | 90.39(8) | N(1)−Pd(1)−P(3) | 101.46(7) |
| N(1)−Pd(1)−P(2) | 162.77(7) | P(2)−Pd(1)−P(3) | 91.31(2) |
| Complex (*R*,*S*)-**14c** | | | |
| Pd(1)−C(1) | 2.043(4) | Pd(1)−P(2) | 2.2653(11) |
| Pd(1)−N(1) | 2.181(4) | Pd(1)−P(1) | 2.4100(11) |
| C(1)−Pd(1)−N(1) | 79.38(16) | C(1)−Pd(1)−P(1) | 170.72(11) |
| C(1)−Pd(1)−P(2) | 92.82(13) | N(1)−Pd(1)−P(1) | 97.97(10) |
| N(1)−Pd(1)−P(2) | 164.42(12) | P(2)−Pd(1)−P(1) | 91.75(4) |
| Complex (*R*,*R*)-**14c** | | | |
| Pd(2)−C(55) | 2.035(4) | Pd(2)−P(4) | 2.2531(10) |
| Pd(2)−N(2) | 2.187(3) | Pd(2)−P(3) | 2.3968(10) |
| C(55)−Pd(2)−N(2) | 78.69(14) | C(55)−Pd(2)−P(3) | 170.27(11) |
| C(55)−Pd(2)−P(4) | 91.36(11) | N(2)−Pd(2)−P(3) | 100.29(9) |
| N(2)−Pd(2)−P(4) | 159.46(10) | P(4)−Pd(2)−P(3) | 92.48(3) |

(29) Mann, B. E.; Taylor, B. F. *$^{13}$C NMR Data for Organometallic Compounds*; Academic Press: London, 1981.

(30) Tschoerner, M.; Kunz, R. W.; Pregosin, P. S. *Magn. Reson. Chem.* **1999**, *37*, 91−97.

(31) Tschoerner, M.; Pregosin, P. S. *Inorg. Chim. Acta* **1999**, *290*, 95−99.

(32) Martinez-Viviente, E.; Pregosin, P. S.; Tschoerner, M. *Magn. Reson. Chem.* **2000**, *38*, 23−28.

(33) Orpen, A. G.; Brammer, L.; Allen, F. H.; Kennard, O.; Watson, D. G.; Taylor, R. *J. Chem. Soc., Dalton Trans.* **1989**, S1−S83.

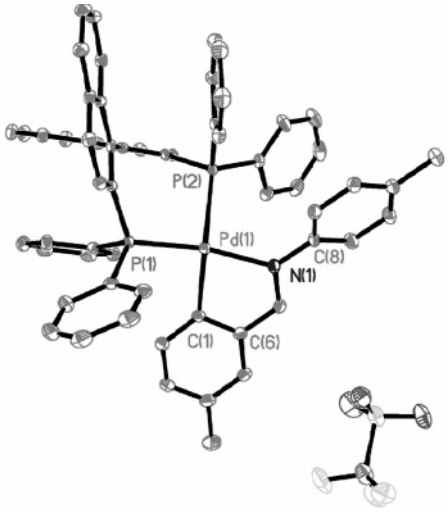


**Figure 1.** ORTEP view of the cation of **8a** with thermal ellipsoids drawn at the 30% probability level (the solvent molecules are omitted for clarity).

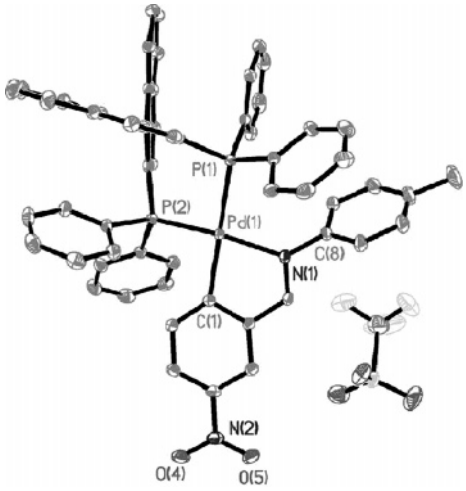


**Figure 2.** ORTEP view of the cation of **10a** with thermal ellipsoids drawn at the 30% probability level (the solvent molecules are omitted for clarity).

3−5 give views of several of the five-membered N,C-chelate rings. As expected, this ring is not planar, and this subject will be extended in the solution discussion.

We note further that the coordinated BINAP ligands demonstrate the usual[34,35] pseudo-axial and pseudo-equatorial P-phenyl rings and that both rings for the Schiff base do not lie in the same plane. Figures 1−4 suggest that the $CF_3SO_3^-$ anion is localized near the nitrogen chelate, and we shall address this point via the HOESY results that follow.

**Overhauser Spectroscopy. (a) Cyclometalated Imine Salts.** Figure 6. shows $^1H,^{19}F$-HOESY results in $CDCl_3$ solution for the model Pd(*rac*-BINAP)(MeO-Schiff base) salts **11a**−**c**, which contain $CF_3SO_3^-$, $BArF^-$, and $PF_6^-$ as anions, respectively. For all three salts there are numerous $^1H,^{19}F$ contacts, and indeed these three differ, but not dramatically. The strongest contacts stem from a number of $PPh_2$ BINAP protons, as previously described.[36] In addition, the relatively small $PF_6^-$ anion (right trace) "sees" the MeO group, the Schiff base ring protons H5, H9, and H10 and the imine proton H7. There is no contact to the aromatic methyl group. This suggests that this anion is trying to position itself close to the partial positive charges on the imine N, Pd, and P atoms. For the slightly larger $CF_3SO_3^-$ anion (left trace) we find contacts to the MeO group, the Schiff base ring protons H2, H3, H5, H9, and H10 and the imine proton H7, plus a number of interactions with the $PPh_2$ BINAP protons. As before, there is no contact to the aromatic methyl group; however, as the triflate is slightly larger and the F atoms somewhat remote from the O atoms bearing the negative charge, we now have contacts to H2 and H3 (see arrow in the figure). These results are consistent with the same type of approach as for the $PF_6^-$ anion. For the even larger $BArF^-$ anion (center trace), we find contacts to the MeO group, the para methyl group, the Schiff base ring protons H2, H3, H5, H9, and H10, and the usual $PPh_2$ BINAP protons; however, the contact to the imine proton H7 is absent. The larger BArF anion, with its meta $CF_3$ groups, stretches far enough to approach the para methyl group but is now slightly further from the imine proton H7. We conclude that in solution, for **8a** and **10a**, the anions prefer to be localized close to the partially positive coordinated imine, Pd, and P moieties. These observations do not reflect directly on the amount of ion pairing (see the diffusion discussion below) but rather on the fact that these anions can approach the cation in a similar way.

**(b) Cyclometalated Amine Salts.** For the chiral amine salts **14a**,**b** and **15a**,**b**, the interpretation of the $^1H,^{19}F$-HOESY results rests on the assignment of the three methyl resonances. The

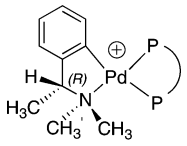


**14**,**15**

correct assignment of the two *N*-methyl groups $CH_3'$ (somewhat closer to the aliphatic methyl) and $CH_3$ (proximate to the methine CH) is crucial, since we expect that the anion may approach the cation via the amine moiety, in analogy to the results described above. The assignment of the aliphatic methyl signal is trivial, as it is spin−spin coupled to the adjacent methine CH and appears as a sharp doublet. The differentiation between $NCH_3'$ and $NCH_3$ was not straightforward and was made primarily using $^1H,^1H$ Overhauser measurements, together with $^{31}P$ spin coupling data. The two *N*-methyl groups reveal very different and characteristic line shapes. $^{31}P,^1H$ correlations (see Figure 7) reveal that the broad "triplet" shape associated with an *N*-methyl group stems from long-range $^{31}P$ spin−spin coupling to two P atoms, and this was interesting but deceptive.[37]

Figure 8 shows NOE results for the (*R*,*S*)- and (*R*,*R*)-BINAP diastereomers **14a**,**b**. The selectivity shown from these NOE data (note the absences indicated by the circles) suggests that the conformation of the five-membered metallacycle ring changes with the chirality of the BINAP. For the *R*,*S* diastere-

(34) (a) Ohta, T. H. T.; Noyori, R. *Inorg. Chem.* **1988**, *27*, 566−569. (b) Mashima, K.; Kusano, K.; Ohta, T.; Noyori, R.; Takaya, H. *J. Chem. Soc., Chem. Commun.* **1989**, 1208. (c) Pathak, D. D.; Adams, H.; Bailey, N. A.; King, P. J.; White, C. *J. Organomet. Chem.* **1994**, *479*, 237. (d) Zhang, X.; Mashima, K.; Koyano, K.; Sayo, N.; Kumobayashi, H.; Akutagawa, S.; Takaya, H. *J. Chem. Soc., Perkin Trans.* **1994**, 2309−2322. (e) Brown, J. M.; Torrente, J. J. P. *Organometallics* **1995**, *14*, 1195−1203. (f) Wiles, J. A.; Lee, C. E.; McDonald, R.; Bergens, S., H. *Organometallics* **1996**, *15*, 3782−3784.

(35) Ruegger, H.; Kunz, R. W.; Ammann, C. J.; Pregosin, P. S. *Magn. Reson. Chem.* **1991**, *29*, 197−203. Ammann, C. J.; Pregosin, P. S.; Ruegger, H.; Albinati, A.; Lianza, F.; Kunz, R. W. *J. Organomet. Chem.* **1992**, *423*, 415−430. Pregosin, P. S.; Rüegger, H.; Salzmann, R.; Albinati, A.; Lianza, F.; Kunz, R. W. *Organometallics* **1994**, *13*, 83−90.

(36) Nama, D.; Schott, D.; Pregosin, P. S.; Veiros, L. F.; Calhorda, M. J. *Organometallics* **2006**, *25*, 4596−4604.

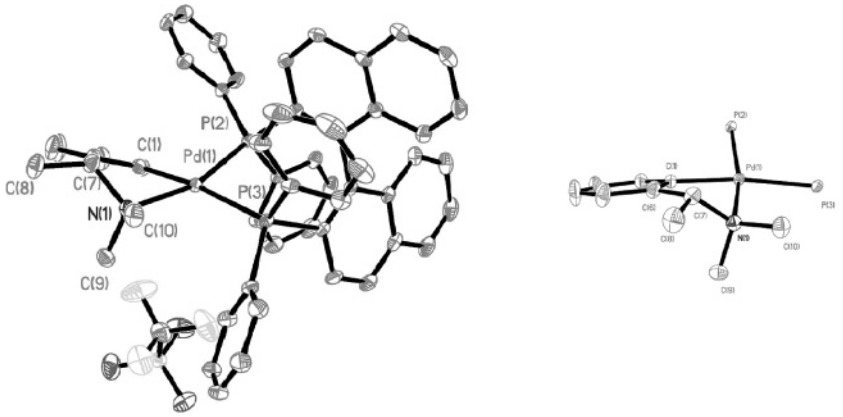


**Figure 3.** (left) ORTEP view of the cation of **14b** with thermal ellipsoids drawn at the 30% probability level and (right) a section showing the five-membered cyclometalated ring.

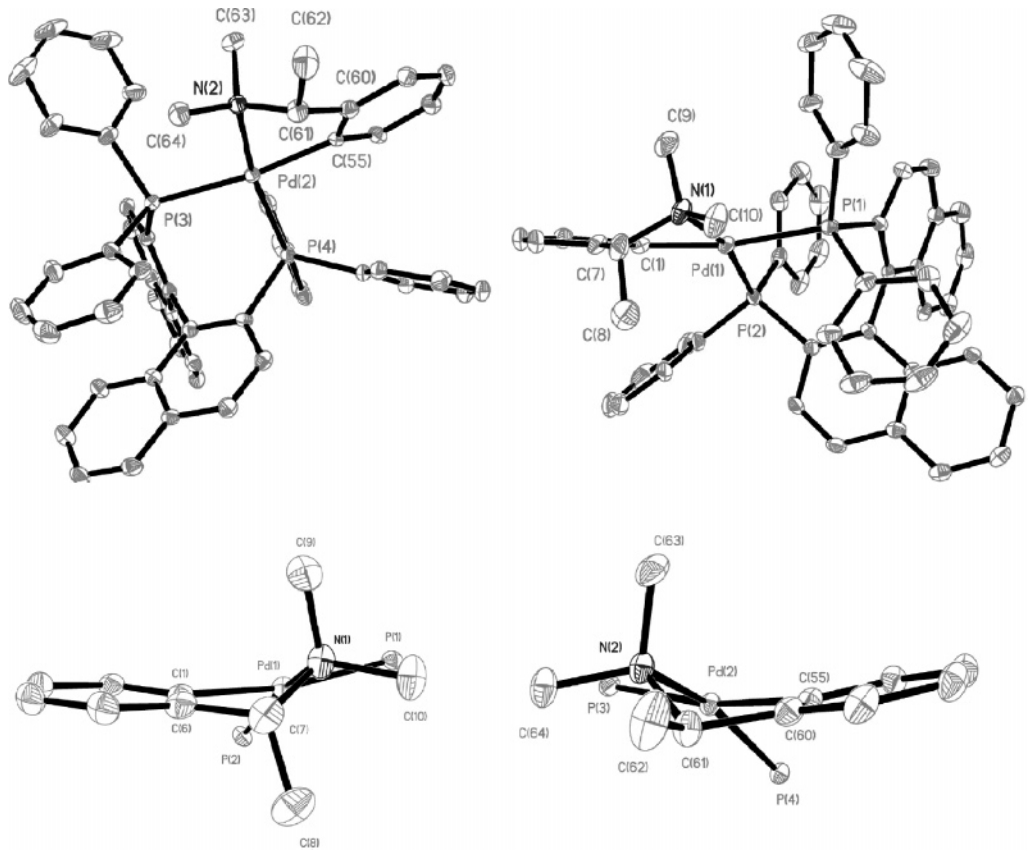


**Figure 4.** (top) ORTEP views of the cations of **14c** with thermal ellipsoids drawn at the 30% probability level and (bottom) sections showing the five-membered cyclometalated rings for the two cations (the anions are not shown for clarity).

omer, the N atom is placed slightly above the plane defined by the Pd and the three carbon atoms, see the sketch in Chart 1). This places the C−Me group in a pseudo-trans position relative to the $NCH_3$ (and thus one finds no NOE between these two groups) but proximate to $NCH_3'$, and the arrow in the sketch indicates this NOE contact. For the *R,R* diastereomer, the N atom is placed slightly below the plane defined by the Pd and the three carbon atoms (see the sketch in Chart 2). This places the C−Me group roughly equidistant from both the $NCH_3$ and the $NCH_3'$ moieties, with the result that two fairly strong

**Chart 1. Structural Fragment of 16**[a]

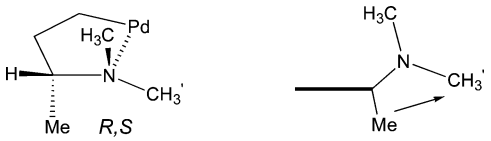


[a] The bold line in the right-hand sketch represents the plane defined by the Pd and the three carbon atoms.

interactions (see arrows) are observed. In line with this proposal are the selective NOE's from the methine CH proton: one each to the $NCH_3$ and the $NCH_3'$ groups in **16** and only one to the $NCH_3$ in **17**. Exactly these two specific ring conformations are found in the solid-state structures, and we show these in Figures 3−5. It is interesting that both amine ring conformations are found for the two diastereomers of the racemic BINAP of **14c**

(37) The difference in the line shape stems from the dependence of $^4J$(P,H) on the relative position of the NMe and NMe′ groups. However, since the change from, for example, (*R*)-BINAP to (*S*)-BINAP changes the amine ring conformation and consequently the relative positions of these two NMe groups, in one diastereomer the NMe appears as a triplet whereas in the other diastereomer the NMe′ is now the triplet.

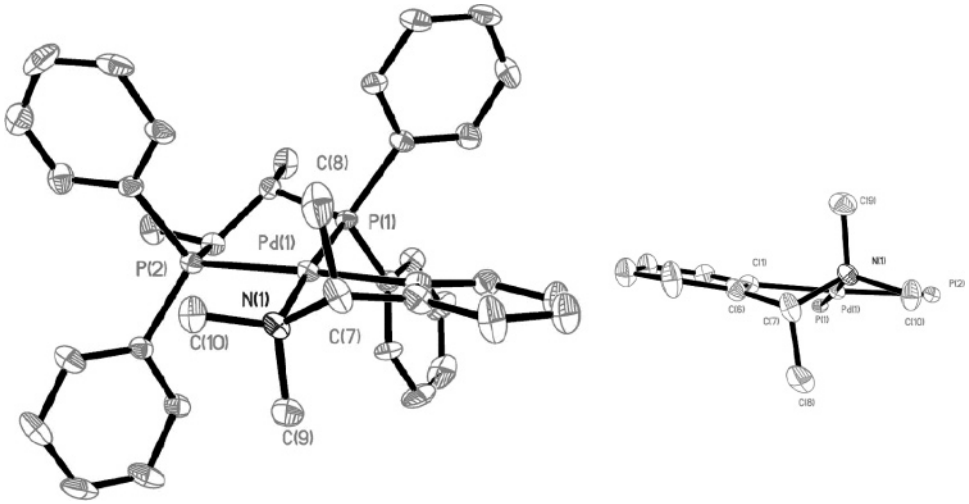


**Figure 5.** ORTEP view of the cation of **15a** with thermal ellipsoids drawn at the 30% probability level and section showing the five-membered cyclometalated ring.

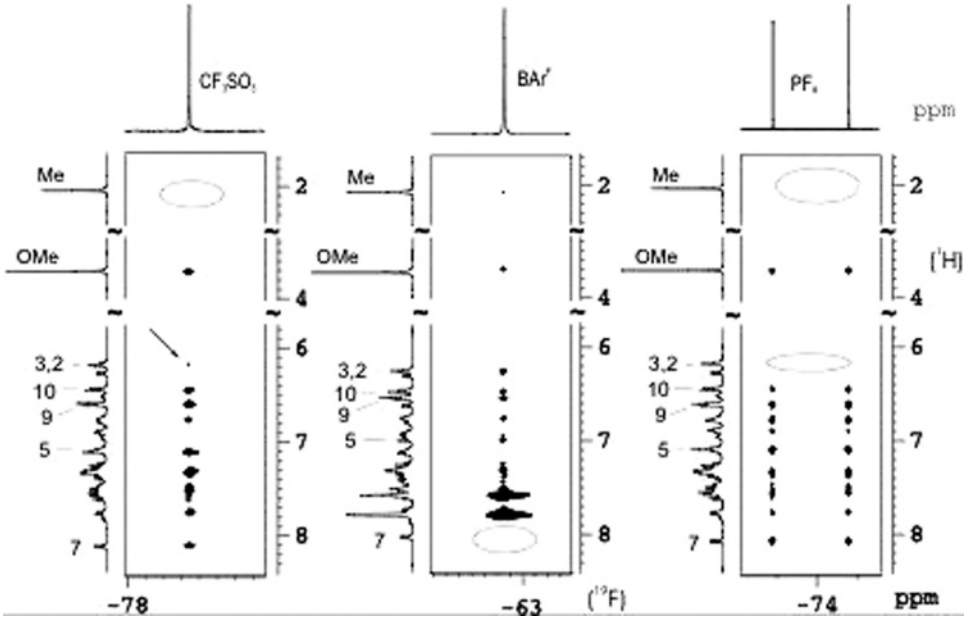


**Figure 6.** $^{1}$H,$^{19}$F HOESY NMR spectra for the complexes **11a** (left), **11b** (middle), and **11c** (right) in $CDCl_3$. The spectra show selective strong contacts primarily to the *P*-phenyl ring protons as well as contacts to the cyclometalated ligand. In complex **11b**, one finds a contact to the para methyl group and not to the imine (H7) proton (400 MHz, 298 K).

(see Figure 4). Moreover, the solid-state data show—if one defines a plane made up of the metal, the two C atoms of the metalated ring C1 and C6, and the methine CH atom C7—that in one diastereomer the N1 atom lies 0.75 Å below this plane, whereas in the second diastereomer, the N2 atom lies 0.87 Å above this plane.

Furthermore, the changes in ring conformation are accompanied by selective anisotropic effects from the *P*-phenyl array on the chemical shifts of the three methyl groups (see Figure 8): e.g., for the *R,R* diastereomer two of these are found at lower frequency. Possibly, this change in amine ring conformation, as a function of the shape of the chiral pocket, relieves unfavorable steric interactions between the $PPh_2$ groups from P2 (trans to the C donor) and the two proximate *N*-methyl groups.

The shapes and relative positions of the chiral arrays containing the four *P*-phenyl groups of complexed (*S*)- and (*R*)-BINAP are shown in **18** and **19**, respectively, and these have been defined by both NMR and X-ray measurements a number of times.[34−36,38,39]

Figure 9 gives the $^{1}$H,$^{19}$F-HOESY results in $CDCl_3$ solution for the BINAP salts **14a**−**c**. The strongest contacts arise from the protons of the *P*-phenyl groups; however, there is a great

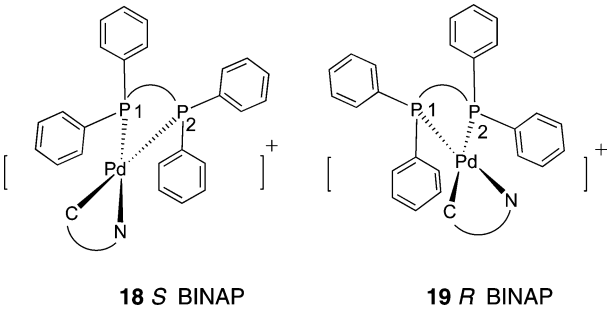


**18** *S* BINAP **19** *R* BINAP

**Chart 2. Structural Fragment of 17**

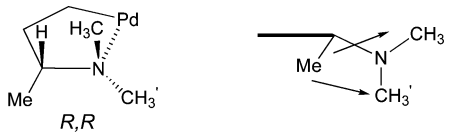

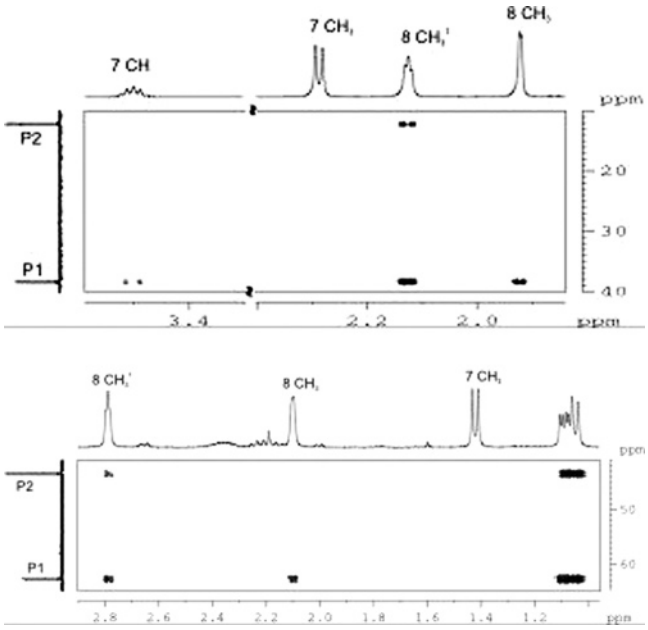


**Figure 7.** Sections of $^{31}$P,$^{1}$H COSY spectra for the complexes (top) **14a** ($CD_2Cl_2$, 500 MHz, 298 K) and (bottom) **15b** ($CDCl_3$, 300 MHz, 298 K), each showing two $^{31}$P contacts to the methyl 8-$CH_3$′ and 8-$CH_3$ respectively, thereby explaining the observed triplet multiplicity.

deal of selectivity. The contacts for (*R*,*R*)-**14b** are not as numerous and are ca. twice as strong as for (*R*,*S*)-**14a**. In **14b**, there are six fairly strong interactions stemming from the methine CH and five aromatic protons of the BINAP and several weaker contacts from the cyclometalated ring.[40] In **14a**, the contact to the methine CH bond in is now *very* weak (and easily missed). For the *R*,*rac* BINAP mixture (far right trace), only the cross-peaks from the $CF_3SO_3^-$ anion to those of the *R*,*R* diastereomer CH and the Me protons are readily observed. This is partly because the strong signals from **14b** mask the weaker ones from **14a**. In any case, the measurement of the racemic mixture, alone, would not have afforded a clear picture of how the triflate anion interacts with the two diastereomeric cations. In summary, these two diastereomers do not show identical $^{1}$H,$^{19}$F-HOESY contacts.

For the Chiraphos diastereomeric pair **15a**,**b**, the $^{1}$H,$^{1}$H NOE's (see the Supporting Information) indicate that, for these salts as well, the nature of the five-membered metallacycle ring changes with the chirality of the Chiraphos ligand. The salt **15a** (*R*,2*S*,3*S*) shows the conformation **16**; however, for the salt **15b** (*R*,2*R*,3*R*) the situation is somewhat different but is in line with the literature.[41] For **15b**, in contrast to **14b**, one finds a somewhat more flexible five-membered-ring conformation on the basis of the observed NOE's.[41] This is interesting and suggests that each enantiomer of BINAP can induce a more decisive conformational change, whereas this is not completely true for both forms of Chiraphos.

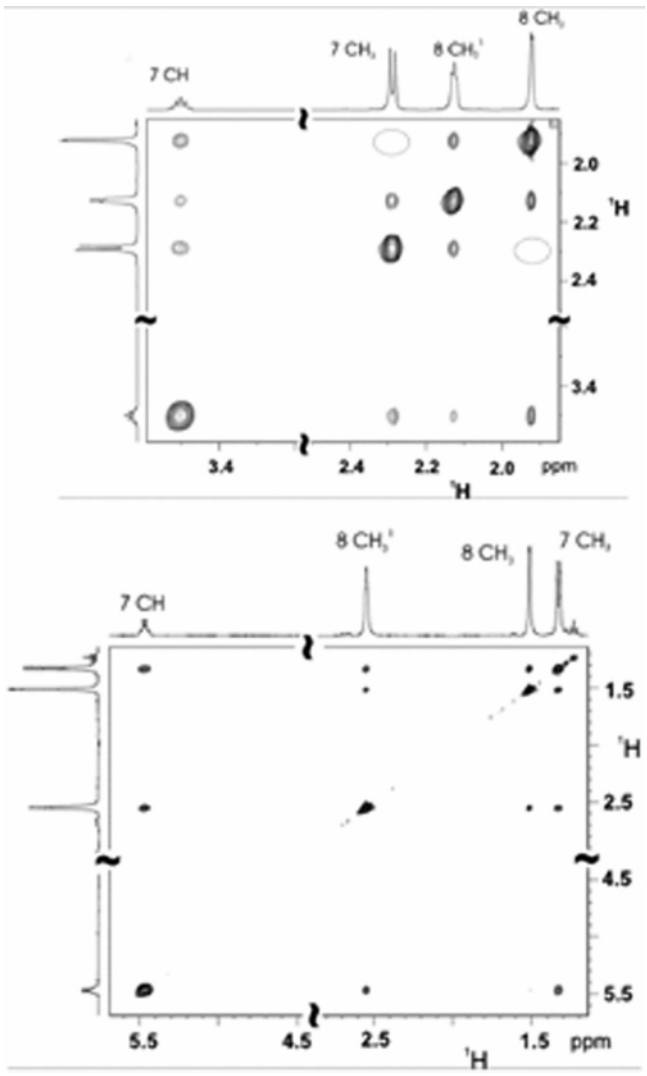


**Figure 8.** Sections of the $^{1}$H,$^{1}$H NOESY spectra for the complexes (top) **14a** ($CD_2Cl_2$, 500 MHz) and (bottom) **14b** ($CDCl_3$, 400 MHz), showing selective NOE contacts in both cases. Blank circles indicate no contact and suggest a specific conformation.

The $^{1}$H,$^{19}$F-HOESY results for the Chiraphos salts **15a**,**b** in $CDCl_3$ solution (Figure 10) are simpler relative to the BINAP analogues. In the *R*,*S*,*S* salt (left trace), one finds major contacts to a *P*-phenyl set and modest cross-peaks[42] arising from the $NCH_3$′ and $NCH_3$ groups. As in **15a**, we do not observe a contact to the methine CH signal. In the *R*,*R*,*R* salt **15b** (right trace) the contacts are more numerous. One finds several strong contacts from the *P*-phenyl groups[42] plus interactions with the *three* methyl groups and the methine CH group. Once again, we observe differences between the diastereomers.

Summarizing this section, we note that the observed $^{1}$H,$^{19}$F HOESY contacts are (a) different for the two Binap-based diastereomers **14a**,**b**, (b) also different for the Chiraphos diastereomeric pair **15a**,**b**, and (c) somewhat similar for **14a** and **15a** (as well as **14b** and **15b**). The source of the difference might involve a different position of the anion, relative to the cation; however, the exact structures are not proven. There are several literature examples in which the anion can be shown to take up specific positions.[16,17e−g]

**Diffusion Data.** Tables 3 and 4 give PGSE diffusion data (*D* values) for the cations and anions of the complexes **8**−**13**

(38) Wiles, J. A.; Bergens, S. H. *Organometallics* **1999**, *18*, 3709−3714.
(39) Drago, D.; Pregosin, P. S.; Tschoerner, M.; Albinati, A. *J. Chem. Soc., Dalton Trans.* **1999**, 2279−2280.
(40) Despite a significant spectroscopic effort, it was not possible to assign each BINAP proton unambiguously. Considerable overlap led to an element of uncertainty with respect to the HOESY contacts.
(41) McFarlane and co-workers (McFarlane, W.; Swarbrick, J. D.; Bookham, J. L. *J. Chem. Soc. Dalton* **1998**, 3233−3238) report (almost) an average of the two conformations for this diastereomer. Our proton spectra and observed NOE results are in agreement with their data. See also Jiang, O.; Rüegger, H.; Venanzi, L. M. *J. Organomet. Chem.* **1995**, *488*, 233−240, for related findings.
(42) There is a very weak contact to the Chiraphos methyl groups. The chiral array does not show marked axial or equatorial *P*-phenyl groups.

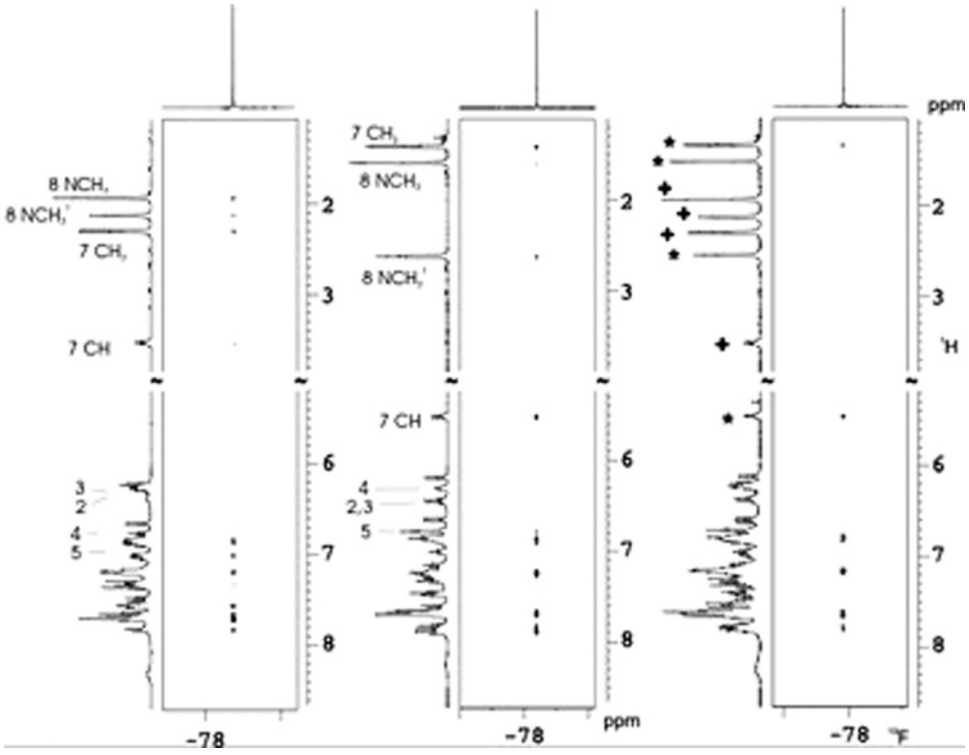


**Figure 9.** $^{1}H,^{19}F$ HOESY spectra for the complexes **14a** (left), **14b** (middle), and **14c** (right, with *rac*-BINAP) in $CDCl_3$, all showing selective strong contacts primarily to the BINAP *P*-phenyl ring protons. One finds medium to weak contacts to the chiral amine cyclometalated ligand protons H7 and H8 in **14a**,**b** and selective contacts in **14c** (400 MHz, 298 K). The stars and crosses in the spectrum of **14c** indicate the signals from the individual diastereomers.

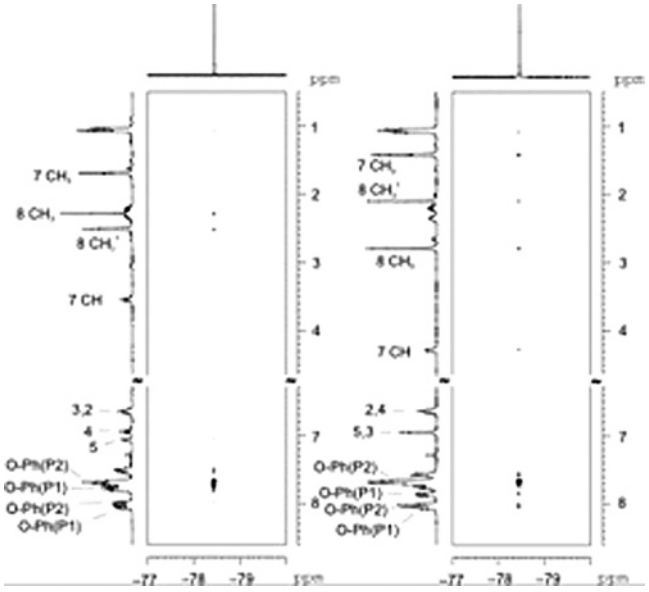


**Figure 10.** $^{1}H,^{19}F$ HOESY spectra for complexes **15a** (left) and **15b** (right) in $CDCl_3$, both showing selective strong contacts primarily to the Chiraphos ortho *P*-phenyl ring protons. One finds selective medium to weak contacts to the chiral amine cyclometalated ligand protons H7 and H8 in **15a**,**b** (400 MHz, 298 K).

and **14** and **15**, respectively, in $CD_2Cl_2$ and $CDCl_3$ solutions. As in previous studies, we assign ca. 100% ion pairing to a salt when the individual *D* values for the cation and anion are identical, within experimental error.[43] In all cases there is much more ion pairing in $CDCl_3$ solution. Further, for **8**−**13**, in $CD_2Cl_2$ solution, the ion pairing seems to be more or less independent of the substituents A and B. For **14** and **15**, we do not find a dependence of the *D* values on the sense of the chirality.

The calculated hydrodynamic radii,[44] $r_H$, are in good agreement with the $r_{X-ray}$ values estimated from the solid-state measurements. From Table 3, one finds that the *D* values for the $CF_3SO_3^-$ and $PF_6^-$ anions are similar, and from Table 4, as expected, it is clear that complexes **14** are somewhat larger than complexes **15**. If we assume an $r_H$ value of ca. 5.9 Å for the solvated BArF anion,[16a] then the ca. $r_H$ value of 6.5 Å for the $BArF^-$ anion in **8**−**13** in $CD_2Cl_2$ solution, given in Table 3, is suggestive of ca. 10% ion pairing: i.e., very modest but not zero ion pairing for this anion. This estimation, in conjunction with the NOE data, serves as a reminder that the observation of strong HOESY contacts does not imply strong ion pairing but, rather, that the anion can approach the cation.

## Conclusions

We find that the chiral organometallic amine chelate recognizes the change in the sense of the chirality, for both the BINAP and the Chiraphos auxiliaries, and responds by a conformational adjustment. Associated with this is a change in the approach of the $CF_3SO_3^-$ anion toward the positively charged centers. The conformational change of the amine ring was easily detected via intramolecular proton−proton NOE data. It was not possible

(43) This assumes (a) that other interactions are absent, e.g., hydrogen bonding, anion encapsulation, etc., which would result in restricted translation of the anion, and (b) that the two ions are markedly different in size.

(44) From the diffusion coefficients it is possible to obtain the so-called hydrodynamic radius, $r_H$, via the Stokes−Einstein equation $r_H = kT/6\pi\eta D$, which, in turn, allows one to estimate the molecular volume. This equation is useful, as it allows one to correct for the solvent viscosity, $\eta$; however, the equation has been criticized, and the literature suggests that the value "6" should be corrected to some smaller value which takes into consideration the volume of the solvent. For a few cases we have made this correction, and these $r_H$ values are given in parenthesis under the values calculated using "6". These "corrected" larger values are likely to be more realistic and are often in better agreement with $r_{X-ray}$.

**Table 3. Diffusion Constants[a] and Radii[b] for Complexes 8−13**

| | $CF_3SO_3^-$ | | | | | BArF$^-$ | | | | $PF_6^-$ | | | |
|---|---|---|---|---|---|---|---|---|---|---|---|---|---|
| | cation ($^1$H) | | | anion ($^{19}$F) | | cation ($^1$H) | | anion ($^{19}$F) | | cation ($^1$H) | | anion ($^{19}$F) | |
| compd | $D$ | $r_H$ ($r_H$) | $r_{X-ray}$ | $D$ | $r_H$ ($r_H$) | $D$ | $r_H$ ($r_H$) | $D$ | $r_H$ | $D$ | $r_H$ ($r_H$) | $D$ | $r_H$ ($r_H$) |
| | | | | | | In $CD_2Cl_2$ | | | | | | | |
| **8** | 7.83 | 6.8 (7.2) | 7.0 | 12.91 | 4.1 (5.0) | 7.54 | 7.0 | 8.14 | 6.5 | | | | |
| **9** | 7.74 | 6.8 | | 12.72 | 4.2 | 7.42 | 7.1 | 8.12 | 6.5 | | | | |
| **10** | 7.73 | 6.8 (7.3) | 7.1 | 12.46 | 4.2 (5.2) | 7.48 | 7.1 (7.5) | 8.20 | 6.5 (7.0) | 7.66 | 6.9 (7.4) | 12.65 | 4.2 (5.1) |
| **11** | 7.69 | 6.9 | | 12.84 | 4.1 | 7.41 | 7.1 | 8.10 | 6.5 | 7.71 | 6.9 | 14.19 | 4.0 |
| **12** | 7.94 | 6.7 | | 12.98 | 4.1 | 7.61 | 7.0 | 8.20 | 6.5 | | | | |
| **13** | 7.75 | 6.8 | | 12.30 | 4.3 | 7.69 | 6.9 | 8.23 | 6.4 | | | | |
| | | | | | | In $CDCl_3$ | | | | | | | |
| **10** | 5.49 | 7.5 (8.0) | | 5.78 | 7.1 (7.6) | 4.85 | 8.5 (8.9) | 5.00 | 8.2 (8.6) | 5.66 | 7.2 (7.8) | 5.95 | 6.9 (7.4) |
| **11** | 5.62 | 7.3 | | 6.06 | 6.8 | 4.95 | 8.3 | 5.21 | 7.9 | 5.68 | 7.2 | 6.15 | 6.7 |

[a] Conditions: 400 MHz, 2 mM. $D$ values are given in $10^{-10}$ m$^2$ s$^{-1}$. [b] $r_H$ values are given in Å; "c" corrected $r_H$ values are given in parentheses. $r_{vdw}$= 2.49 Å ($CD_2Cl_2$), $r_{vdw}$= 2.60 Å ($CDCl_3$), $\eta(CH_2Cl_2) = 0.414 \times 10^{-3}$ kg m$^{-1}$ s$^{-1}$, $\eta(CHCl_3) = 0.534 \times 10^{-3}$ kg m$^{-1}$ s$^{-1}$ at 299 K.

**Table 4. Diffusion Constants[a] and Radii[b] for Complexes 14 and 15 in $CD_2Cl_2$ and in $CDCl_3$.**

| | | $CD_2Cl_2$ | | | | | $CDCl_3$ | | | |
|---|---|---|---|---|---|---|---|---|---|---|
| | | cation ($^1$H) | | | anion ($^{19}$F) | | cation ($^1$H) | | anion ($^{19}$F) | |
| compd | config[c] | $D$ | $r_H$ ($r_H$) | $r_{X-ray}$ | $D$ | $r_H$ ($r_H$) | $D$ | $r_H$ ($r_H$) | $D$ | $r_H$ ($r_H$) |
| **14** | **a** (*R*,*S*) | 8.24 | 6.4 | | 13.04 | 4.1 | 5.86 | 7.0 | 6.27 | 6.5 |
| | **b** (*R*,*R*) | 8.16 | 6.5 (7.0) | 6.9 | 12.58 | 4.2 (5.1) | 5.97 | 6.9 (7.4) | 6.17 | 6.6 (7.2) |
| | **c** (*R*,*rac*) | 8.11 | 6.5 | | 13.04 | 4.1 | 5.97 | 6.9 | 6.24 | 6.6 |
| | | 8.18 | 6.5 | | | | 5.88 | 7.0 | | |
| **15** | **a** (*R*,2*S*,3*S*) | 8.86 | 6.0 (6.5) | | 12.70 | 4.2 (5.1) | 6.30 | 6.5 (7.1) | 6.68 | 6.1 (6.8) |
| | **b** (*R*,2*R*,3*R*) | 8.86 | 6.0 | | 12.65 | 4.2 | 6.30 | 6.5 | 6.53 | 6.2 |

[a] Conditions: 400 MHz, 2 mM. $D$ values are given in $10^{-10}$ m$^2$ s$^{-1}$. [b] $r_H$ values are given in Å; "c" corrected $r_H$ values are given in parentheses. $r_{vdw}$ = 2.49 Å ($CD_2Cl_2$), $r_{vdw}$ = 2.60 Å ($CDCl_3$), $\eta(CH_2Cl_2) = 0.414 \times 10^{-3}$ kg m$^{-1}$ s$^{-1}$, $\eta(CHCl_3) = 0.534 \times 10^{-3}$ kg m$^{-1}$ s$^{-1}$ at 299 K. [c] The first configuration refers to the asymmetric carbon in the cyclometalated ring, and the second configuration refers to the BINAP ring.

to unambiguously define the interplay between the anion and cation, although some interesting selectivity exists.

We believe that the NOE observations will eventually prove helpful in understanding how chiral auxiliaries affect structural changes and thus influence the outcome of enantioselective reactions. It is now well documented that a prochiral substrate, e.g., an olefin capable of forming a chelate ring, may complex either the *re* or *si* face and that the chiral pocket assists in this selection process. However, it is not obvious that the chiral pocket might be able to induce a change in the conformation of such a chelate ring. Further, from this and earlier studies, it is now becoming clear that noncoordinating anions (a) can be selective in their approach to a metal center and (b) do not all demonstrate the same degree of ion pairing—and this is especially true for the commonly used BArF$^-$ anion.

## Experimental Section

**General Comments**. All air-sensitive manipulations were carried out under a nitrogen atmosphere. All solvents were dried over an appropriate drying agent and then distilled under nitrogen. Deuterated solvents were dried by distillation over molecular sieves and stored under nitrogen. The ligands *rac*-BINAP (Strem), (*R*)-BINAP and (*S*)-BINAP (Alfa Aesar), (*R*)-(+)-*N*,*N*-dimethyl-1-phenylethylamine (Aldrich), (2*R*,3*R*)-Chiraphos and (2*S*,3*S*)-Chiraphos (Acros), and silver salts (Aldrich) were purchased from commercial sources and used as received. The chloro-bridged metal complexes $(PdClL)_2$ (**1**−**6**; L = cyclometalated ligands (Schiff base)), and the *R* or *S N*,*N*-dimethyl-1-phenylethylamine complex **7** were synthesized according to known literature procedures.[45,46] The complexes **14** and **15** have been reported by Noyori[26a] and McFarlane, respectively.[41] $^1$H, $^{31}$P, $^{13}$C, $^{19}$F, and 2D NMR spectra were recorded with Bruker DPX-250, 300, 400, 500, and 700 MHz spectrometers at room temperature unless otherwise noted. Elemental analysis and mass spectra were performed at the ETH Zürich.

**Diffusion Measurements.** All of the PGSE measurements were carried out using the stimulated echo pulse sequence and performed on a 400 MHz Bruker Avance spectrometer, equipped with a microprocessor-controlled gradient unit and a multinuclear inverse probe with an actively shielded Z-gradient coil. The shape of the gradient pulse was rectangular, and its length was 1.75 ms. The gradient strength was incremented in 4% steps from 4% to 60%, so that 12−15 points could be used for regression analysis. The time between midpoints of the gradients was 167.75 ms, and the gradient recovery time was set at 100 $\mu$s for all experiments. All of the diffusion $^1$H spectra were acquired using 16K points, 16 transients, a 5 s relaxation delay, and a 1.5 s acquisition time. All of the $^{19}$F spectra were acquired using 16K points, 16 or 8 transients, a relaxation delay of $5T_1$ (approximately 15−20 s), and a 4 s acquisition time. Spin−lattice relaxation times ($T_1$) were measured using the standard inversion−recovery method. Both the $^1$H and $^{19}$F diffusion experiments were processed using Bruker software with an exponential multiplication (EM) window function and a line broadening of 1.0 Hz. The measurements were carried out without spinning at a set temperature of 299 K within the NMR probe. As indicated in Tables 3 and 4, diffusion values were measured on 2 mM $CD_2Cl_2$ and $CDCl_3$ solutions. Cation diffusion rates were measured using the $^1$H signal from the methyl protons of either the *N*,*N*-dimethyl-1-phenylethylamine or Schiff base. Anion diffusion data were obtained from the $^{19}$F resonances. The solvent viscosities used for the calculation of $r_H$ were 0.414 and 0.534 for $CD_2Cl_2$ and $CDCl_3$, respectively.

**NOE Measurements.** The $^1$H,$^1$H NOESY NMR experiments were acquired by the standard three-pulse sequence (noesyph) using a 600 ms or 1 s relaxation delay and a 600 ms mixing time on a Bruker spectrometer at a set temperature of 298 K with phase cycling by the TPPI method. Typically, 16 transients (DS 16) were acquired into 2K data points for each of the 512 values of $t_1$. A

(45) Albinati, A.; Pregosin, P. S.; Ruedi, R. *Helv. Chim. Acta* **1985**, *68*, 2046−2061.

(46) Cope, A. C.; Friedrich, E. C. *J. Am. Chem. Soc.* **1968**, *90*, 909.

QSINE weighting function was used in each dimension prior to Fourier transformation into a 2K × 1K data matrix. The spectral width in each dimension was 5000 Hz, and the transmitter was set at the center of the range. The $^{19}$F,$^{1}$H-HOESY NMR experiments were acquired using the standard four-pulse sequence (invhoesy) with either a 600 or 800 ms mixing time. The doubly tuned TXI probe head of the 400 MHz spectrometer was set at 298 K. The experiment was carried out using phase cycling by the TPPI method (pulse width: F1, 4000 Hz; F2, 1132.2 Hz). Typically, 16 transients (DS 4) were acquired into 2K data points for each of the 512 or 1 K values of $t_1$. A QSINE and EM weighting functions (F1 and F2 dimensions, respectively) were used prior to Fourier transformation into a 2K × 1K data matrix. The delay between increments was set to 2 s.

**[Pd(*rac*-BINAP)($C_{15}H_{14}N$)][$CF_3SO_3$] (8a).** To 1 equiv of [Pd($\mu$-Cl)($C_{15}H_{14}N$)]$_2$ (33.4 mg, 700.3 g mol$^{-1}$, 47.7 × 10$^{-3}$ mol) were added 2 equiv of *rac*-BINAP (59.4 mg, 622.67 g mol$^{-1}$, 95.4 × 10$^{-3}$ mol) and 2 equiv of AgOTf (24.5 mg, 256.94 g mol$^{-1}$, 95.4 × 10$^{-3}$ mol) in dichloromethane. The reaction mixture was stirred at 25 °C for 3 h. The resulting yellow solution was separated from the solid and reduced in vacuo. The product was recrystallized by dissolving in the minimum volume of dichloromethane and layering with hexane, affording **8a** as yellow crystals. Yield of [$C_{60}H_{46}F_3NO_3P_2PdS$] (**8a**): 90 mg, 0.083 mol, 87%. Anal. Found (calcd) for [Pd(*rac*-BINAP)($C_{15}H_{14}N$)][$CF_3SO_3$]·$H_2O$: C, 65.16 (65.25); H, 4.35 (4.38); N, 1.27 (1.27). $^1$H NMR ($CD_2Cl_2$, 400 MHz, 25 °C): $\delta$ 1.62 (s, 3H), 2.07 (s, 3H), 6.15−7.78 (m, aromatic), 8.06 (dd, $^4J_{HP-trans}$ = 6.4 Hz, $^4J_{HP-cis}$ = 1.0 Hz). $^{31}$P{$^1$H} NMR ($CD_2Cl_2$, 161 MHz, 25 °C): $\delta$ 13.5 (d, AB spin, $^2J_{PP}$ = 47 Hz), 41.1 (d, AB spin, $^2J_{PP}$ = 47 Hz). $^{19}$F NMR ($CD_2Cl_2$, 376.5 MHz, 25 °C): $\delta$ −79.3 (s). $^{13}$C{$^1$H} NMR ($CD_2Cl_2$, 100 MHz, 25 °C): $\delta$ 20.6 (s, $CH_3$), 20.8 (s, Me), 115.4−178.0 (aromatic), 180.0 (t, =*C*H, $^1J_{CP}$ = 4.2 Hz). MS (MALDI; *m*/*z*): M$^+$ 938.2.

**[Pd(*rac*-BINAP)($C_{15}H_{14}N$)][$BAr^F$] (8b).** To 1 equiv of [Pd($\mu$-Cl)($C_{15}H_{14}N$)]$_2$ (21.5 mg, 700.3 g mol$^{-1}$, 30.7 × 10$^{-3}$ mol) were added 2 equiv of *rac*-BINAP (38.2 mg, 622.67 g mol$^{-1}$, 61.4 × 10$^{-3}$ mol) and 2 equiv of NaBArF (54.4 mg, 886.21 g mol$^{-1}$, 61.4 × 10$^{-3}$ mol) in dichloromethane. The reaction mixture was stirred at 25 °C for 3 h. The resulting yellow solution was separated from the solid and reduced in vacuo. Yield of [$C_{91}H_{58}BF_{24}NP_2Pd$] (**8b**): 104 mg, 0.0578 mol, 94%). Anal. Found (calcd) for [Pd(*rac*-BINAP)($C_{15}H_{14}N$)][$BAr^F$]: C, 60.98 (60.70); H, 3.43 (3.25); N, 0.79 (0.78). $^1$H NMR ($CD_2Cl_2$, 400 MHz, 25 °C): $\delta$ 2.06 (s, 3H), 2.17 (s, 3H), 6.15−8.30 (m, aromatic), 8.05 (d, $^4J_{HP-trans}$ = 6.9 Hz). $^{31}$P{$^1$H} NMR ($CD_2Cl_2$, 161 MHz, 25 °C): $\delta$ 13.4 (d, AB spin, $^2J_{PP}$ = 48 Hz), 41.1 (d, AB spin, $^2J_{PP}$ = 48 Hz). $^{19}$F NMR ($CD_2Cl_2$, 376.5 MHz, 25 °C): $\delta$ −63.3 (s). $^{13}$C{$^1$H} NMR ($CD_2Cl_2$, 100 MHz, 25 °C): $\delta$ 20.5 (s, $CH_3$), 20.8 (s, Me), 115.4−178.0 (aromatic), 179.9 (t, =*C*H, $^1J_{CP}$ = 3.5 Hz). MS (MALDI; *m*/*z*): M$^+$ 938.2.

**[Pd(*rac*-BINAP)($C_{14}H_{11}ClN$)][$CF_3SO_3$] (9a).** To 1 equiv of [Pd($\mu$-Cl)($C_{14}H_{11}ClN$)]$_2$ (28.3 mg, 741.14 g mol$^{-1}$, 38.2 × 10$^{-3}$ mol) were added 2 equiv of *rac*-BINAP (47.5 mg, 622.67 g mol$^{-1}$, 76.4 × 10$^{-3}$ mol) and 2 equiv of AgOTf (19.6 mg, 256.94 g mol$^{-1}$, 76.4 × 10$^{-3}$ mol) in dichloromethane. The reaction mixture was stirred at 25 °C for 3 h. The resulting yellow solution was separated from the solid and reduced in vacuo. Yield of [$C_{59}H_{43}ClF_3NO_3P_2PdS$] (**9a**): 80 mg, 0.072 mol, 94%. Anal. Found (calcd) for [Pd(*rac*-BINAP)($C_{14}H_{11}ClN$)][$CF_3SO_3$]: C, 63.04 (64.02); H, 4.03 (3.92); N, 1.21 (1.27). $^1$H NMR ($CD_2Cl_2$, 400 MHz, 25 °C): 2.07 (s, 3H), 6.15−7.78 (m, aromatic), 8.08 (dd, 1H, $^4J_{HP-trans}$ = 6.4 Hz, $^4J_{HP-cis}$ = 1.0 Hz). $^{31}$P{$^1$H} NMR ($CD_2Cl_2$, 161 MHz, 25 °C): $\delta$ 13.7 (d, AB spin, $^2J_{PP}$ = 47 Hz), 40.6 (d, AB spin, $^2J_{PP}$ = 47 Hz). $^{19}$F NMR ($CD_2Cl_2$, 376.5 MHz, 25 °C): $\delta$ −79.3 (s). $^{13}$C-{$^1$H} NMR ($CD_2Cl_2$, 100 MHz, 25 °C): $\delta$ 20.8 (s, $CH_3$), $\delta$ 115.4−178.0 (aromatic), 178.3 (t, =*C*H, $^1J_{CP}$ = 4.1 Hz). MS (MALDI; *m*/*z*): M$^+$ 958.2.

**[Pd(*rac*-BINAP)($C_{14}H_{11}ClN$)][$BAr^F$] (9b).** To 1 equiv of [Pd($\mu$-Cl)($C_{14}H_{11}ClN$)]$_2$ (19.6 mg, 741.14 g mol$^{-1}$, 30.7 × 10$^{-3}$ mol) were added 2 equiv of *rac*-BINAP (32.9 mg, 622.67 g mol$^{-1}$, 53.0 × 10$^{-3}$ mol) and 2 equiv of NaBArF (46.8 mg, 886.21 g mol$^{-1}$, 53.0 × 10$^{-3}$ mol) in dichloromethane. The reaction mixture was stirred at 25 °C for 3 h. The resulting yellow solution was separated from the solid and reduced in vacuo. Yield of [$C_{90}H_{55}BClF_{24}NP_2$-Pd] (**9b**): 91 mg, 0.0499 mol, 94%. Anal. Found (calcd) for [Pd(*rac*-BINAP)($C_{14}H_{11}ClN$)][$BAr^F$]: C, 59.38 (59.36); H, 3.25 (3.04); N, 0.82 (0.77). $^1$H NMR ($CD_2Cl_2$, 400 MHz, 25 °C): $\delta$ 2.07 (s, 3H), 6.15−8.30 (m, aromatic), 8.06 (d, $^4J_{HP-trans}$ = 6.0 Hz). $^{31}$P-{$^1$H} NMR ($CD_2Cl_2$, 161 MHz, 25 °C): $\delta$ 13.7 (d, AB spin, $^2J_{PP}$ = 47 Hz), 40.8 (d, AB spin, $^2J_{PP}$ = 47 Hz). $^{19}$F NMR ($CD_2Cl_2$, 376.5 MHz, 25 °C): $\delta$ −63.3 (s). $^{13}$C{$^1$H} NMR ($CD_2Cl_2$, 100 MHz, 25 °C): $\delta$ 20.8 (s, $CH_3$), 115.4−178.0 (aromatic), 178.8 (t, =*C*H, $^1J_{CP}$ = 4.0 Hz). MS (MALDI; *m*/*z*): M$^+$ 958.2.

**[Pd(*rac*-BINAP)($C_{14}H_{11}N_2O_2$)][$CF_3SO_3$] (10a).** To 1 equiv of [Pd($\mu$-Cl)($C_{14}H_{11}N_2O_2$)]$_2$ (29.3 mg, 762.24 g mol$^{-1}$, 38.4 × 10$^{-3}$ mol) were added 2 equiv of *rac*-BINAP (47.9 mg, 622.67 g mol$^{-1}$, 76.9 × 10$^{-3}$ mol) and 2 equiv of AgOTf (19.8 mg, 256.94 g mol$^{-1}$, 76.9 × 10$^{-3}$ mol) in dichloromethane. The reaction mixture was stirred at 25 °C for 3 h. The resulting yellow solution was separated from the solid and reduced in vacuo. The product was recrystallized by dissolving in the minimum volume of dichloromethane and layering with hexane, affording **10a** as yellow crystals. Yield of [$C_{59}H_{43}F_3N_2O_5P_2PdS$] (**10a**): 79 mg, 0.071 mol, 92%. Anal. Found (calcd) for [Pd(*rac*-BINAP)($C_{14}H_{11}N_2O_2$)][$CF_3SO_3$]: C, 62.89 (63.42); H, 4.12 (3.88); N, 2.51 (2.51). $^1$H NMR ($CD_2Cl_2$, 400 MHz, 25 °C): 2.09 (s, 3H), 6.15−8.30 (m, aromatic), 8.26 (dd, $^4J_{HP-trans}$ = 6.4 Hz). $^{31}$P{$^1$H} NMR ($CD_2Cl_2$, 161 MHz, 25 °C): $\delta$ 14.1 (d, AB spin, $^2J_{PP}$ = 47 Hz), 40.1 (d, AB spin, $^2J_{PP}$ = 47 Hz). $^{19}$F NMR ($CD_2Cl_2$, 376.5 MHz, 25 °C): $\delta$ −79.3 (s). $^{13}$C{$^1$H} NMR ($CD_2$-$Cl_2$, 100 MHz, 25 °C): $\delta$ 20.9 (s, $CH_3$), $\delta$ 115.4−178.0 (aromatic), 178.6 (t, =*C*H, $^1J_{CP}$ = 3.7 Hz). MS (MALDI; *m*/*z*): M$^+$ 969.1.

**[Pd(*rac*-BINAP)($C_{14}H_{11}N_2O_2$)][$BAr^F$] (10b).** To 1 equiv of [Pd($\mu$-Cl)($C_{14}H_{11}N_2O_2$)]$_2$ (22.0 mg, 762.24 g mol$^{-1}$, 28.9 × 10$^{-3}$ mol) were added 2 equiv of *rac*-BINAP (35.9 mg, 622.67 g mol$^{-1}$, 57.7 × 10$^{-3}$ mol) and 2 equiv of NaBArF (51.2 mg, 886.21 g mol$^{-1}$, 57.7 × 10$^{-3}$ mol) in dichloromethane. The reaction mixture was stirred at 25 °C for 3 h. The resulting yellow solution was separated from the solid and reduced in vacuo. Yield of [$C_{90}H_{55}BF_{24}N_2O_2P_2$-Pd] (**10b**): 100 mg, 0.0546 mol, 94%. Anal. Found (calcd) for [Pd(*rac*-BINAP)($C_{14}H_{11}N_2O_2$)][$BAr^F$]: C, 58.92 (59.02); H, 3.31 (3.03); N, 1.57 (1.53). $^1$H NMR ($CD_2Cl_2$, 400 MHz, 25 °C): $\delta$ 2.08 (s, 3H), 6.15−8.30 (m, aromatic), 8.23 (d, $^4J_{HP-trans}$ = 6.8 Hz, $^4J_{HP-cis}$ = 1.2 Hz). $^{31}$P{$^1$H} NMR ($CD_2Cl_2$, 161 MHz, 25 °C): $\delta$ 14.1 (d, AB spin, $^2J_{PP}$ = 47 Hz), 40.1 (d, AB spin, $^2J_{PP}$ = 47 Hz). $^{19}$F NMR ($CD_2Cl_2$, 282 MHz, 25 °C): $\delta$ −63.3 (s). $^{13}$C{$^1$H} NMR ($CD_2Cl_2$, 100 MHz, 25 °C): $\delta$ 20.8 (s, $CH_3$), $\delta$ 115.4−178.0 (aromatic), 178.4 (t, =*C*H, $^1J_{CP}$ = 3.9 Hz). MS (MALDI; *m*/*z*): M$^+$ 969.2.

**[Pd(*rac*-BINAP)($C_{14}H_{11}N_2O_2$)][$PF_6$] (10c).** To 1 equiv of [Pd($\mu$-Cl)($C_{14}H_{11}N_2O_2$)]$_2$ (19.6 mg, 732.36 g mol$^{-1}$, 25.7 × 10$^{-3}$ mol) were added 2 equiv of *rac*-BINAP (32.0 mg, 622.67 g mol$^{-1}$, 51.4 × 10$^{-3}$ mol) and 2 equiv of $NH_4PF_6$ (8.4 mg, 163 g mol$^{-1}$, 51.4 × 10$^{-3}$ mol) in acetone. The reaction mixture was stirred at 25 °C for 2 h. Water was then added and the mixture stirred for a further 1 h. The resulting precipitate was filtered off and dried in vacuo. Yield of [$C_{58}H_{43}F_6N_2O_2P_3Pd$] (**10c**): 51 mg, 0.0458 mol, 89%. Anal. Found (calcd) for [Pd(*rac*-BINAP)($C_{14}H_{11}N_2O_2$)][$PF_6$]: C, 62.28 (62.57); H, 3.97 (3.89); N, 2.48 (2.52). $^1$H NMR ($CDCl_3$, 400 MHz, 25 °C): $\delta$ 2.1 (s, 3H), 6.30−8.25 (m, aromatic), 8.25 (d, 1H, $^4J_{HP-trans}$ = 6.8 Hz). $^{31}$P{$^1$H} NMR ($CDCl_3$, 161 MHz, 25 °C): $\delta$ 14.1 (d, AB spin, $^2J_{PP}$ = 46 Hz), 40.1 (d, AB spin, $^2J_{PP}$ = 46 Hz), −143.2 (sep, $^1J_{PF}$ = 713 Hz). $^{19}$F NMR ($CDCl_3$, 376.5 MHz, 25 °C): $\delta$ −73.8 (d, $^1J_{FP}$ = 713 Hz). $^{13}$C{$^1$H} NMR ($CDCl_3$,

100 MHz, 25 °C): $\delta$ 20.8 (s, $CH_3$), 115.4−178.0 (aromatic), 178.5 (t, =*C*H, $^1J_{CP}$ = 3.9 Hz). MS (MALDI; *m*/*z*): $M^+$ 969.1.

**[Pd(*rac*-BINAP)($C_{15}H_{14}NO$)][$CF_3SO_3$] (11a).** To 1 equiv of [Pd($\mu$-Cl)($C_{15}H_{14}NO$)]$_2$ (17.4 mg, 732.3 g mol$^{-1}$, 24.0 × 10$^{-3}$ mol) were added 2 equiv of *rac*-BINAP (29.6 mg, 622.67 g mol$^{-1}$, 48.0 × 10$^{-3}$ mol) and 2 equiv of AgOTf (12.3 mg, 256.94 g mol$^{-1}$, 48.0 × 10$^{-3}$ mol) in dichloromethane. The reaction mixture was stirred at 25 °C for 3 h. The resulting yellow solution was separated from the solid and reduced in vacuo. Yield of [$C_{60}H_{46}F_3NO_4P_2$PdS] (**11a**): 54 mg, 0.049 mol, 98%. $^1$H NMR ($CDCl_3$, 400 MHz, 25 °C): $\delta$ 2.03 (s, 3H), 3.71 (s, 3H), 6.15−7.78 (m, aromatic), 8.07 (d, 1H, $^4J_{HP-trans}$ = 6.4 Hz). $^{31}$P{$^1$H} NMR ($CDCl_3$, 161 MHz, 25 °C): $\delta$ 13.6 (d, AB spin, $^2J_{PP}$ = 47 Hz), 41.2 (d, AB spin, $^2J_{PP}$ = 47 Hz), −142.9 (sep, $^1J_{PF}$ = 713 Hz). $^{19}$F NMR ($CDCl_3$, 376.5 MHz, 25 °C): $\delta$ −73.8 (d, $^1J_{FP}$ = 713 Hz). $^{13}$C{$^1$H} NMR ($CDCl_3$, 100 MHz, 25 °C): $\delta$ 21.4 (s, $CH_3$), 55.8 (s, OMe), 115.4−178.0 (aromatic), 180.0 (t, =*C*H, $^1J_{CP}$ = 4.1 Hz). MS (MALDI; *m*/*z*): $M^+$ 954.2.

**[Pd(*rac*-BINAP)($C_{15}H_{14}NO$)][$BAr^F$] (11b).** To 1 equiv of [Pd($\mu$-Cl)($C_{15}H_{14}NO$)]$_2$ (21.7 mg, 732.36 g mol$^{-1}$, 29.6 × 10$^{-3}$ mol) were added 2 equiv of *rac*-BINAP (36.9 mg, 622.67 g mol$^{-1}$, 59.3 × 10$^{-3}$ mol) and 2 equiv of NaBArF (52.5 mg, 886.21 g mol$^{-1}$, 59.3 × 10$^{-3}$ mol) in dichloromethane. The reaction mixture was stirred at 25 °C for 3 h. The resulting yellow solution was separated from the solid and reduced in vacuo. Yield of [$C_{91}H_{58}BF_{24}NOP_2$Pd] (**11b**): 100 mg, 0.055 mol, 92%. Anal. Found (calcd) for [Pd(*rac*-BINAP)($C_{15}H_{14}NO$)][$BAr^F$]: C, 60.17 (60.29); H, 3.22 (3.38); N, 0.77 (0.78). $^1$H NMR ($CDCl_3$, 400 MHz, 25 °C): $\delta$ 2.03 (s, 3H), 3.70 (s, 3H), 6.15−7.78 (m, aromatic), 7.95 (d, $^4J_{HP-trans}$ = 6.4 Hz). $^{31}$P{$^1$H} NMR ($CDCl_3$, 161 MHz, 25 °C): $\delta$ 13.4 (d, AB spin, $^2J_{PP}$ = 47 Hz), 41.2 (d, AB spin, $^2J_{PP}$ = 47 Hz). $^{19}$F NMR ($CDCl_3$, 376.5 MHz, 25 °C): $\delta$ −62.4 (s). $^{13}$C{$^1$H} NMR ($CDCl_3$, 100 MHz, 25 °C): $\delta$ 21.4 (s, $CH_3$), 55.8 (s, OMe), 115.4−178.0 (aromatic), 180.0 (t, =*C*H, $^1J_{CP}$ = 4.0 Hz). MS (MALDI; *m*/*z*): $M^+$ 954.2.

**[Pd(*rac*-BINAP)($C_{15}H_{14}NO$)][$PF_6$] (11c).** To 1 equiv of [Pd($\mu$-Cl)($C_{15}H_{14}NO$)]$_2$ (18.3 mg, 732.36 g mol$^{-1}$, 25.0 × 10$^{-3}$ mol) were added 2 equiv of *rac*-BINAP (31.1 mg, 622.67 g mol$^{-1}$, 50.0 × 10$^{-3}$ mol) and 2 equiv of $NH_4PF_6$ (8.15 mg, 163 g mol$^{-1}$, 50.0 × 10$^{-3}$ mol) in acetone. The reaction mixture was stirred at 25 °C for 2 h. Water was then added and the mixture stirred for a further 1 h. The resulting precipitate was filtered off and dried in vacuo. Yield of [$C_{59}H_{46}F_6NOP_3$Pd] (**11c**): 44 mg, 0.044 mol, 80%. Anal. Found (calcd) for [Pd(*rac*-BINAP)($C_{15}H_{14}NO$)][$PF_6$]: C, 64.52 (64.67); H, 4.22 (4.39); N, 1.28 (1.29). $^1$H NMR ($CDCl_3$, 400 MHz, 25 °C): $\delta$ 2.03 (s, 3H), 3.71 (s, 3H), 6.15−7.78 (m, aromatic), 8.07 (d, $^4J_{HP-trans}$ = 6.4 Hz). $^{31}$P{$^1$H} NMR ($CDCl_3$, 161 MHz, 25 °C): $\delta$ 13.6 (d, AB spin, $^2J_{PP}$ = 47 Hz), 41.2 (d, AB spin, $^2J_{PP}$ = 47 Hz), −142.9 (sep, $^1J_{PF}$ = 713 Hz). $^{19}$F NMR ($CDCl_3$, 376.5 MHz, 25 °C): $\delta$ −73.8 (d, $^1J_{FP}$ = 713 Hz). $^{13}$C{$^1$H} NMR ($CDCl_3$, 100 MHz, 25 °C): $\delta$ 21.4 (s, $CH_3$), 55.8 (s, OMe), 115.4−178.0 (aromatic), 180.0 (t, =*C*H, $^1J_{CP}$ = 4.1 Hz). MS (MALDI; *m*/*z*): $M^+$ 954.2.

**[Pd(*rac*-BINAP)($C_{15}H_{14}N$)][$CF_3SO_3$] (12a).** To 1 equiv of [Pd($\mu$-Cl)($C_{15}H_{14}N$)]$_2$ (20.1 mg, 700.3 g mol$^{-1}$, 28.7 × 10$^{-3}$ mol) were added 2 equiv of *rac*-BINAP (35.7 mg, 622.67 g mol$^{-1}$, 57.4 × 10$^{-3}$ mol) and 2 equiv of AgOTf (14.7 mg, 256.94 g mol$^{-1}$, 57.4 × 10$^{-3}$ mol) in dichloromethane. The reaction mixture was stirred at 25 °C for 3 h. The resulting yellow solution was separated from the solid and reduced in vacuo. Yield of [$C_{60}H_{46}F_3NO_3P_2$PdS] (**12a**): 112 mg, 0.103 mol, 90%. $^1$H NMR ($CD_2Cl_2$, 400 MHz, 25 °C): $\delta$ 1.69 (s, 3H), 2.07 (s, 3H), 6.15−7.78 (m, aromatic), 8.05 (dd, 1H, $^4J_{HP-trans}$ = 6.9 Hz, $^4J_{HP-cis}$ = 1.0 Hz). $^{31}$P{$^1$H} NMR ($CD_2Cl_2$, 161 MHz, 25 °C): $\delta$ 13.3 (d, AB spin, $^2J_{PP}$ = 48 Hz), 40.8 (d, AB spin, $^2J_{PP}$ = 48 Hz). $^{19}$F NMR ($CD_2Cl_2$, 376.5 MHz, 25 °C): $\delta$ −79.3 (s). $^{13}$C{$^1$H} NMR ($CD_2Cl_2$, 100 MHz, 25 °C): $\delta$ 20.8 (s, $CH_3$), 21.8 (s, Me), 115.4−178.0 (aromatic), 180.0 (t, =*C*H, $^1J_{CP}$ = 4.6 Hz). MS (MALDI; *m*/*z*): $M^+$ 938.2.

**[Pd(*rac*-BINAP)($C_{15}H_{14}N$)][$BAr^F$] (12b).** To 1 equiv of [Pd($\mu$-Cl)($C_{15}H_{14}N$)]$_2$ (22.3 mg, 700.3 g mol$^{-1}$, 31.8 × 10$^{-3}$ mol) were added 2 equiv of the *rac*-BINAP (39.7 mg, 622.67 g mol$^{-1}$, 63.7 × 10$^{-3}$ mol) and 2 equiv of NaBArF (56.4 mg, 886.21 g mol$^{-1}$, 63.7 × 10$^{-3}$ mol) in dichloromethane. The reaction mixture was stirred at 25 °C for 3 h. The resulting yellow solution was separated from the solid and reduced *in vacuo*. [$C_{91}H_{58}BF_{24}NP_2$Pd] **12b** (Yield: 101 mg, 0.0561mol, 88%). Anal. Found (calcd) for [Pd(*rac*-BINAP)($C_{15}H_{14}N$)][$BAr^F$] C {61.27 (60.70)} H {3.34 (3.25)} N {0.78 (0.78)} $^1$H NMR ($CD_2Cl_2$, 400 MHz, 25 °C): $\delta$ 2.06 (s, 3H), 2.38 (s, 3H), 6.15−8.30 (m, aromatic), 8.02 (d, $^4J_{HP-trans}$ = 6.9 Hz). $^{31}$P{$^1$H} NMR ($CD_2Cl_2$, 161 MHz, 25 °C): $\delta$ 13.3 (d, AB spin, $^2J_{PP}$ = 48 Hz), 40.8 (d, AB spin, $^2J_{PP}$ = 48 Hz). $^{19}$F NMR ($CD_2Cl_2$, 376.5 MHz, 25 °C): $\delta$ −63.3 (s). $^{13}$C{$^1$H} NMR ($CD_2Cl_2$, 100 MHz, 25 °C): $\delta$ 20.3 (s, $CH_3$), 21.3 (s, Me), 115.4−178.0 (aromatic), 179.1 (t, =*C*H, $^1J_{CP}$ = 4.1 Hz). MS (MALDI; *m*/*z*): $M^+$ 938.2.

**[Pd(*rac*-BINAP)($C_{14}H_{11}N_2O_2$)][$CF_3SO_3$] (13a).** To 1 equiv of [Pd($\mu$-Cl)($C_{14}H_{11}N_2O_2$)]$_2$ (29.0 mg, 762.24 g mol$^{-1}$, 38.0 × 10$^{-3}$ mol) were added 2 equiv of *rac*-BINAP (47.4 mg, 622.67 g mol$^{-1}$, 76.0 × 10$^{-3}$ mol) and 2 equiv of AgOTf (19.6 mg, 256.94 g mol$^{-1}$, 76.0 × 10$^{-3}$ mol) in dichloromethane. The reaction mixture was stirred at 25 °C for 3 h. The resulting yellow solution was separated from the solid and reduced in vacuo. Yield of [$C_{59}H_{43}F_3N_2O_5P_2$PdS] (**13a**): 80 mg, 0.071 mol, 94%. Anal. Found (calcd) for [Pd(*rac*-BINAP)($C_{14}H_{11}ClN$)][$CF_3SO_3$]: C, 62.80 (63.42); H, 4.04 (3.88); N, 2.54 (2.51). $^1$H NMR ($CD_2Cl_2$, 400 MHz, 25 °C): $\delta$ 2.09 (s, 3H), 6.15−8.30 (m, aromatic), 8.29 (d, 1H, $^4J_{HP-trans}$ = 6.8 Hz). $^{31}$P{$^1$H} NMR ($CD_2Cl_2$, 161 MHz, 25 °C): $\delta$ 14.3 (d, AB spin, $^2J_{PP}$ = 47 Hz), 39.9 (d, AB spin, $^2J_{PP}$ = 47 Hz). $^{19}$F NMR ($CD_2Cl_2$, 376.5 MHz, 25 °C): $\delta$ −79.3 (s). $^{13}$C{$^1$H} NMR ($CD_2Cl_2$, 100 MHz, 25 °C): $\delta$ 20.9 (s, $CH_3$), 115.4−178.0 (aromatic), 178.8 (t, =*C*H, $^1J_{CP}$ = 3.8 Hz). MS (MALDI; *m*/*z*): $M^+$ 969.2.

**[Pd(*rac*-BINAP)($C_{14}H_{11}N_2O_2$)][$BAr^F$] (13b).** To 1 equiv of [Pd($\mu$-Cl)($C_{14}H_{11}N_2O_2$)]$_2$ (21.5 mg, 762.24 g mol$^{-1}$, 28.2 × 10$^{-3}$ mol) were added 2 equiv of *rac*-BINAP (35.1 mg, 622.67 g mol$^{-1}$, 56.4 × 10$^{-3}$ mol) and 2 equiv of NaBArF (50.0 mg, 886.21 g mol$^{-1}$, 56.4 × 10$^{-3}$ mol) in dichloromethane. The reaction mixture was stirred at 25 °C for 3 h. The resulting yellow solution was separated from the solid and reduced in vacuo. Yield of [$C_{90}H_{55}BF_{24}N_2O_2P_2$Pd] (**13b**): 92 mg, 0.0502 mol, 89%. Anal. Found (calcd) for [Pd(*rac*-BINAP)($C_{14}H_{11}N_2O_2$)][$BAr^F$]: C, 59.29 (59.02); H, 3.08 (3.03); N, 1.60 (1.53). $^1$H NMR ($CD_2Cl_2$, 400 MHz, 25 °C): $\delta$ 2.09 (s, 3H), 6.15−8.30 (m, aromatic), 8.23 (d, $^4J_{HP-trans}$ = 6.8 Hz). $^{31}$P{$^1$H} NMR ($CD_2Cl_2$, 161 MHz, 25 °C): $\delta$ 14.3 (d, AB spin, $^2J_{PP}$ = 46 Hz), 39.9 (d, AB spin, $^2J_{PP}$ = 46 Hz). $^{19}$F NMR ($CD_2Cl_2$, 282 MHz, 25 °C): $\delta$ −63.3 (s). $^{13}$C{$^1$H} NMR ($CD_2Cl_2$, 100 MHz, 25 °C): $\delta$ 20.8 (s, $CH_3$), 115.4−178.0 (aromatic), 178.2 (t, =*C*H, $^1J_{CP}$ = 3.8 Hz). MS (MALDI; *m*/*z*): $M^+$ 969.1.

**[Pd((*S*)-BINAP)((*R*)-$C_{10}H_{14}N$)][$CF_3SO_3$] (14a).** To 1 equiv of [Pd($\mu$-Cl)($C_{10}H_{14}N$)]$_2$ (30.3 mg, 600.35 g mol$^{-1}$, 50.5 × 10$^{-3}$ mol) were added 2 equiv of (*S*)-BINAP (62.8 mg, 622.67 g mol$^{-1}$, 110.9 × 10$^{-3}$ mol) and 2 equiv of AgOTf (25.9 mg, 256.94 g mol$^{-1}$, 110.9 × 10$^{-3}$ mol) in dichloromethane. The reaction mixture was stirred at 25 °C for 3 h. The resulting yellow solution was separated from the solid and reduced in vacuo. Yield of [$C_{55}H_{46}F_3NO_3P_2$PdS] (**14a**): 102 mg, 98%. $^1$H NMR ($CD_2Cl_2$, 500 MHz, 25 °C): 1.92 (d, 3H, $^4J_{PH}$ = 2.1 Hz), 2.12 (br t, 3H, $^4J_{PH}$ = 3.5 Hz), 2.28 (d, 2H, $^3J_{HH}$ = 6.3 Hz), 3.49 (m, 1H), 6.15−8.50 (m, aromatic). $^{31}$P{$^1$H} NMR ($CD_2Cl_2$, 283 MHz, 25 °C): $\delta$ 11.1 (d, AB spin, $^2J_{PP}$ = 43 Hz), 38.2 (d, AB spin, $^2J_{PP}$ = 43 Hz). $^{19}$F NMR ($CD_2Cl_2$, 282.4 MHz, 25 °C): $\delta$ −78.8 (s). $^{13}$C{$^1$H} NMR ($CD_2Cl_2$, 125.8 MHz, 25 °C): $\delta$ 9.0 (s, $CH_3$), 25.9 (s, $CH_3$), 40.3 (s, $NCH_3$),

**Table 5. Crystal Data and Strucure Refinement Details for 8a, 10a, and 14b,c**

| | 8a | 10a | 14b | 14c |
|---|---|---|---|---|
| color, shape | yellow, cube | yellow, cube | yellow, cube | yellow, needle |
| empirical formula | $C_{63}H_{50}Cl_5F_3NO_3P_2PdS$ | $C_{62}H_{49}Cl_6F_3N_2O_5P_2PdS$ | $C_{57}H_{47}Cl_6F_3NO_3P_2PdS$ | $C_{110}H_{92}F_6N_2O_6P_4Pd_2S_2$ |
| formula wt | 1303.69 | 1372.13 | 1264.06 | 2052.66 |
| temp (K) | 200(2) | 200(2) | 200(2) | 200(2) |
| cryst syst | triclinic | Triclinic | orthorhombic | monoclinic |
| space group | $P\bar{1}$ | $P\bar{1}$ | $P2_12_12_1$ | $P2_1$ |
| $a$ (Å) | 11.3820(11) | 13.2269(5) | 11.8308(10) | 17.6911(10) |
| $b$ (Å) | 15.5502(14) | 14.3139(6) | 12.8673(10) | 11.5190(6) |
| $c$ (Å) | 17.1910(16) | 16.4955(7) | 36.642(3) | 23.0571(13) |
| α (deg) | 71.786(2) | 75.4480(10) | 90.00 | 90.00 |
| $\beta$ (deg) | 84.497(2) | 82.3430(10) | 90.00 | 90.8320(10) |
| $\gamma$ (deg) | 79.695(2) | 85.9830(10) | 90.00 | 90.00 |
| $V$ (Å$^3$) | 2841.0(5) | 2993.7 (2) | 5578.0(8) | 4698.2(4) |
| $Z$ | 2 | 2 | 4 | 2 |
| calcd density (Mg m$^3$) | 1.524 | 1.522 | 1.505 | 1.451 |
| abs coeff (mm$^{-1}$) | 0.713 | 0.727 | 0.770 | 0.566 |
| $F$(000) | 1326 | 1392 | 2564 | 2104 |
| cryst size (mm) | 0.49 × 0.27 × 0.19 | 0.54 × 0.28 × 0.27 | 0.51 × 0.48 × 0.28 | 0.51 × 0.46 × 0.40 |
| min, max $\theta$ (deg) | 1.57, 26.02 | 1.47, 28.36 | 1.68, 28.33 | 0.88, 28.33 |
| index ranges | $-14 \le h \le 14$<br>$-19 \le k \le 19$<br>$-21 \le l \le 21$ | $-17 \le h \le 17$<br>$-19 \le k \le 19$<br>$-22 \le l \le 22$ | $-15 \le h \le 15$<br>$-17 \le k \le 17$<br>$-48 \le l \le 48$ | $-23 \le h \le 23$<br>$-15 < \le k \le 15$<br>$-30 \le l \le 29$ |
| no. of rflns collected | 25 009 | 55 615 | 58 341 | 49 277 |
| no. of indep rflns, $R$(int) | 11 160, 0.0246 | 14 874, 0.0361 | 13 866, 0.0345 | 23 207, 0.0342 |
| no. of data/restraints/params | 11 160/0/712 | 14 874/0/739 | 13 866/0/687 | 23 207/1/1189 |
| goodness of fit on $F^2$ | 1.034 | 1.040 | 1.078 | 1.043 |
| final R1, wR2 indices ($I > 2\sigma(I)$) | 0.0572, 0.1462 | 0.0465, 0.1241 | 0.0371, 0.0918 | 0.0505, 0.1151 |
| final R1, wR2 indices (all data) | 0.0639, 0.1538 | 0.0540, 0.1306 | 0.0394, 0.0930 | 0.0577, 0.1199 |
| largest diff peak, hole/e Å$^{-3}$ | 2.956, −2.584 | 1.785, −1.123 | 0.882, −0.598 | 1.605, −1.209 |

46.7 (s, $NCH_3$), 49.5 (s, $NCH_3$), 51.5 (s, $NCH_3$), 74.4 (m, CH), 79.8 (m, CH), 115.4−180.0 (aromatic). MS (MALDI; *m*/*z*): $M^+$ 876.2.

**[Pd((*R*)-BINAP)((*R*)-$C_{10}H_{14}N$)][$CF_3SO_3$] (14b).** To 1 equiv of [Pd($\mu$-Cl)($C_{10}H_{14}N$)]$_2$ (30.0 mg, 600.35 g mol$^{-1}$, 49.9 × 10$^{-3}$ mol) were added 2 equiv of (*R*)-BINAP (62.2 mg, 622.67 g mol$^{-1}$, 99.9 × 10$^{-3}$ mol) and 2 equiv of AgOTf (25.7 mg, 256.94 g mol$^{-1}$, 99.9 × 10$^{-3}$ mol) in dichloromethane. The reaction mixture was stirred at 25 °C for 3 h. The resulting yellow solution was separated from the solid and reduced in vacuo. Yield of [$C_{55}H_{46}F_3NO_3P_2PdS$] (**14b**): 100 mg, 97%. $^1$H NMR ($CDCl_3$, 400 MHz, 25 °C): 1.33 (d, 2H, $^3J_{HH}$ = 6.3 Hz), 1.51 (d, 3H, $^4J_{PH}$ = 2.1 Hz), 2.54, (br t, 3H, $^4J_{PH}$ = 3.5 Hz), 5.46 (m, 1H), 6.15−8.50 (m, aromatic). $^{31}$P-{$^1$H} NMR ($CDCl_3$, 161.9 MHz, 25 °C): $\delta$ 11.1 (d, AB spin, $^2J_{PP}$ = 43 Hz), 38.2 (d, AB spin, $^2J_{PP}$ = 43 Hz); $^{19}$F NMR ($CD_2Cl_2$, 282.4 MHz, 25 °C): $\delta$ −78.8 (s); $^{13}$C{$^1$H} NMR ($CD_2Cl_2$, 125.8 MHz, 25 °C): $\delta$ 9.0 (s, $CH_3$), 40.3 (s, $NCH_3$), 49.5 (s, $NCH_3$), 74.4 (m, CH), 115.4−180.0 (aromatic). MS (MALDI; *m*/*z*): $M^+$ 876.2.

**[Pd(*rac*-BINAP)((*R*)-$C_{10}H_{14}N$)][$CF_3SO_3$] (14c).** To 1 equiv of [Pd($\mu$-Cl)($C_{10}H_{14}N$)]$_2$ (33.6 mg, 600.35 g mol$^{-1}$, 55.9 × 10$^{-3}$ mol) were added 2 equiv of *rac*-BINAP (69.7 mg, 622.67 g mol$^{-1}$, 111.9 × 10$^{-3}$ mol) and 2 equiv of AgOTf (28.8 mg, 256.94 g mol$^{-1}$, 111.9 × 10$^{-3}$ mol) in dichloromethane. The reaction mixture was stirred at 25 °C for 3 h. The resulting yellow solution was separated from the solid and reduced in vacuo. Yield of [$C_{55}H_{46}F_3NO_3P_2PdS$] (**14c**): 111 mg, 0.108 mol, 96%. $^1$H NMR ($CD_2Cl_2$, 700 MHz, 25 °C): 1.35 (d, 2H, $^3J_{HH}$ = 6.3 Hz), 1.53 (d, 3H, $^4J_{PH}$ = 2.1 Hz), 1.92 (d, 3H, $^4J_{PH}$ = 2.1 Hz), 2.12 (br t, 3H, $^4J_{PH}$ = 3.5 Hz), 2.28 (d, 2H, $^3J_{HH}$ = 6.3 Hz), 2.51 (br t, 3H, $^4J_{PH}$ = 3.5 Hz), 3.49 (m, 1H), 5.19 (m, 1H), 6.15−8.50 (m, aromatic). $^{31}$P{$^1$H} NMR ($CD_2Cl_2$, 283 MHz, 25 °C): $\delta$ 10.5 (d, AB spin, $^2J_{PP}$ = 44.2 Hz), 11.1 (d, AB spin, $^2J_{PP}$ = 43 Hz), 37.2 (d, AB spin, $^2J_{PP}$ = 44.2 Hz), 38.2 (d, AB spin, $^2J_{PP}$ = 43 Hz). $^{19}$F NMR ($CD_2Cl_2$, 282.4 MHz, 25 °C): $\delta$ −78.8 (s). $^{13}$C{$^1$H} NMR ($CD_2Cl_2$, 175 MHz, 25 °C): $\delta$ 25.9 (s, $CH_3$), 46.7 (s, $NCH_3$), 51.5 (s, $NCH_3$), 79.8 (m, CH), 115.4−180.0 (aromatic). MS (MALDI; *m*/*z*): $M^+$ 876.2.

**[Pd(2*S*,3*S*)-Chiraphos)((*R*)-$C_{10}H_{14}N$)][$CF_3SO_3$] (15a).** To 1 equiv of [Pd($\mu$-Cl)($C_{10}H_{14}N$)]$_2$ (28.7 mg, 600.35 g mol$^{-1}$, 47.8 × 10$^{-3}$ mol) were added 2 equiv of (2*S*,3*S*)-Chiraphos (40.8 mg, 426.47 g mol$^{-1}$, 95.6 × 10$^{-3}$ mol) and 2 equiv of AgOTf (24.6 mg, 256.94 g mol$^{-1}$, 95.6 × 10$^{-3}$ mol) in dichloromethane. The reaction mixture was stirred at 25 °C for 3 h. The resulting colorless solution was separated from the solid and reduced in vacuo. Yield of [$C_{39}H_{42}F_3NO_3P_2PdS$] (**15a**): 80 mg, 98%. $^1$H NMR ($CDCl_3$, 400 MHz, 25 °C): 1.05 (dd, 3H, $^3J_{HH}$ = 6.4 Hz, $^3J_{PH}$ = 2.4 Hz), 1.07 (d, 3H, $^3J_{HH}$ = 6.4 Hz), 1.69 (d, 3H, $^3J_{HH}$ = 6.4 Hz), 2.22 (m, 1H), 2.28 (d, 3H, $^4J_{PH}$ = 1.2 Hz), 2.31 (m, 1H), 2.50 (t, 3H, $^4J_{PH}$ = 3.6 Hz), 3.55 (m, 1H), 6.50−8.20 (m, aromatic). $^{31}$P{$^1$H} NMR ($CDCl_3$, 161.9 MHz, 25 °C): $\delta$ 45.2 (d, AB spin, $^2J_{PP}$ = 40 Hz), 63.3 (d, AB spin, $^2J_{PP}$ = 40 Hz). $^{19}$F NMR ($CDCl_3$, 376.5 MHz, 25 °C): $\delta$ −78.4 (s). $^{13}$C{$^1$H} NMR ($CDCl_3$, 100 MHz, 25 °C): $\delta$ 13.9 (dd, $CH_3$, $^2J_{CP}$ = 17.1 Hz, $^3J_{CP}$ = 6.1 Hz), 15.4 (dd, $CH_3$, $^2J_{CP}$ = 18.6 Hz, $^3J_{CP}$ = 5.5 Hz), 26.6 (s, $CH_3$), 38.4 (dd, CH, $^1J_{CP}$ = 26.8 Hz, $^2J_{CP}$ = 13.4 Hz), 39.9 (dd, CH, $^1J_{CP}$ = 33.3 Hz, $^2J_{CP}$ = 22 Hz), 50.4 (d, $NCH_3$, $^3J_{CP}$ = 5.2 Hz), 51.7 (d, $NCH_3$, $^3J_{CP}$ = 2.4 Hz), 78.8 (br t, CH), 115.4−180.0 (aromatic). MS (MALDI; *m*/*z*): $M^+$ 680.2.

**[Pd(2*R*,3*R*)-Chiraphos)((*R*)-$C_{10}H_{14}N$)][$CF_3SO_3$] (15b).** To 1 equiv of [Pd($\mu$-Cl)($C_{10}H_{14}N$)]$_2$ (30.5 mg, 600.35 g mol$^{-1}$, 50.8 × 10$^{-3}$ mol) were added 2 equiv of (2*R*,3*R*)-Chiraphos (43.3 mg, 426.47 g mol$^{-1}$, 101.6 × 10$^{-3}$ mol) and 2 equiv of AgOTf (26.1 mg, 256.94 g mol$^{-1}$, 101.6 × 10$^{-3}$ mol) in dichloromethane. The reaction mixture was stirred at 25 °C for 3 h. The resulting colorless solution was separated from the solid and reduced in vacuo. Yield of [$C_{39}H_{42}F_3NO_3P_2PdS$] (**15b**): 80 mg, 95%. $^1$H NMR ($CDCl_3$, 300 MHz, 25 °C): 1.04 (dd, 3H, $^3J_{HH}$ = 6.8 Hz, $^3J_{PH}$ = 2.9 Hz), 1.08 (d, 3H, $^3J_{HH}$ = 6.7 Hz), 1.41 (d, 3H, $^3J_{HH}$ = 6.7 Hz), 2.09 (d, 3H, $^4J_{PH}$ = 1.6 Hz), 2.22 (m, 1H), 2.35 (m, 1H), 2.78 (t, 3H, $^4J_{PH}$ = 2.5 Hz), 4.31 (m, 1H), 6.50−8.20 (m, aromatic). $^{31}$P{$^1$H} NMR ($CDCl_3$, 121.5 MHz, 25 °C): $\delta$ 43.3 (d, AB spin, $^2J_{PP}$ = 40.5 Hz), 62.5 (d, AB spin, $^2J_{PP}$ = 40.5 Hz). $^{19}$F NMR ($CDCl_3$, 376.5 MHz, 25 °C): $\delta$ −78.5 (s). $^{13}$C{$^1$H} NMR ($CDCl_3$, 100 MHz, 25 °C): $\delta$ 14.1 (dd, $CH_3$, $^2J_{CP}$ = 16.2 Hz, $^3J_{CP}$ = 6.0 Hz), 15.4 (dd, $CH_3$, $^2J_{CP}$ = 17.8 Hz, $^3J_{CP}$ = 5.2 Hz), 16.6 (s, $CH_3$), $\delta$ 38.6 (dd, CH, $^1J_{CP}$ = 26.5 Hz, $^2J_{CP}$ = 12.7 Hz), 40.8 (dd, CH, $^1J_{CP}$ = 33.1 Hz, $^2J_{CP}$ = 21.5 Hz), 45.7 (s, $NCH_3$), $\delta$ 52.1 (s, $NCH_3$), 75.4 (t, CH, $^3J_{CP}$ = 3.2 Hz), 115.4−180.0 (aromatic). MS (MALDI; *m*/*z*): $M^+$ 680.3.

**Solid-State Measurements**. X-ray structural measurements were carried out on a Bruker CCD diffractometer: Bruker SMART PLATFORM, with CCD detector, graphite monochromator, Mo Kα (0.710 73 Å) radiation and a low-temperature device (200 K). Crystals of **8**, **10**, and **14a**,**c**, suitable for X-ray diffraction, were obtained by crystallization from a saturated $CH_2Cl_2$/hexane solution at low temperature. The single crystals were mounted in a poly(perfluoroalkyl ether) oil on top of a glass fiber and fixed with some epoxy glue. Calculations were performed on a PC system with SHELXTL (version 6.12) and SHELXL-97 (G. M. Sheldrick, Göttingen, Germany, 1997). The structures were solved by either Patterson (**8**, **10**, **14c**) or direct (**10**) methods and successive interpretation of the difference Fourier maps, followed by full-matrix least-squares refinement (against $F^2$). Non-hydrogen atoms were refined freely with anisotropic displacement parameters. The contribution of the hydrogen atoms, in their calculated positions, was included in the refinement using a riding model for the X-ray structures. Moreover, an empirical absorption correction using SADABS (version 2.03) was applied to all structures. The dichloromethane solvent found in the structure of **14a** is disordered, and the chlorine atoms were placed in two positions, each with an occupancy of 50%, to achieve a satisfactory wR2 value.

Selected interatomic distances and bond angles are reported in Table 2. Relevant data concerning crystallographic data, data collection, and refinement details are compiled in Table 5. Further details of the crystallographic studies have been deposited with the Cambridge Crystallographic Data Centre: CCDC Nos. 640811−640814 for **8**, **10**, and **14a**,**c**, respectively.

**Acknowledgment.** P.S.P. thanks the Swiss National Science Foundation and the ETH Zurich for support, as well as the Johnson Matthey Organization for the loan of palladium salts. Special thanks are due to Dr. H. Rüegger for his advice and help.

**Supporting Information Available:** Figures giving NOE spectra for **15a** and **15b** and CIF files giving complete crystallographic data. This material is available free of charge via the Internet at http://pubs.acs.org.

OM700299B